

See discussions, stats, and author profiles for this publication at: <https://www.researchgate.net/publication/15541607>

Structure-Based Design of Novel HIV Protease Inhibitors: Carboxamide-Containing 4-Hydroxycoumarins and 4-Hydroxy-2-pyrones as Potent Nonpeptidic Inhibitors

ARTICLE *in* JOURNAL OF MEDICINAL CHEMISTRY · OCTOBER 1995

Impact Factor: 5.45 · DOI: 10.1021/jm00018a023 · Source: PubMed

CITATIONS

83

READS

36

10 AUTHORS, INCLUDING:



Alfredo G Tomasselli

Independent Pharmaceuticals Professional

103 PUBLICATIONS 4,859 CITATIONS

SEE PROFILE

Structure-Based Design of Novel HIV Protease Inhibitors: Carboxamide-Containing 4-Hydroxycoumarins and 4-Hydroxy-2-pyrone as Potent Nonpeptidic Inhibitors

Suvit Thaisrivongs,^{*,†} Keith D. Watenpaugh,[‡] W. Jeffrey Howe,[§] Paul K. Tomich,^{||} Lester A. Dolak,^{||} Kong-Teck Chong,[†] Che-Shen C. Tomich,[†] Alfredo G. Tomasselli,[#] Steve R. Turner,[†] Joseph W. Strohbach,[†] Anne M. Mulichak,[‡] Musiri N. Janakiraman,[‡] Joseph B. Moon,[§] Janet C. Lynn,^{||} Miao-Miao Horng,^{||} Roger R. Hinshaw,[†] Kimberly A. Curry,[†] and Donna J. Rothrock[#]

Medicinal Chemistry Research, Physical & Analytical Chemistry, Computer-Aided Drug Discovery, Chemical & Biological Screen, Cancer & Infectious Diseases Research, Molecular Biology, and Biochemistry, Upjohn Laboratories, Kalamazoo, Michigan 49001

Received April 21, 1995[§]

The low oral bioavailability and rapid biliary excretion of peptide-derived HIV protease inhibitors have limited their utility as potential therapeutic agents. Our broad screening program to discover nonpeptidic HIV protease inhibitors had previously identified compound **II** (phenprocoumon, $K_i = 1 \mu\text{M}$) as a lead template. Crystal structures of HIV protease complexes containing the peptide-derived inhibitor **I** (1-(naphthoxyacetyl)-L-histidyl-5(S)-amino-6-cyclohexyl-3(R),4(R)-dihydroxy-2(R)-isopropylhexanoyl-L-isoleucine *N*-(2-pyridylmethyl)amide) and nonpeptidic inhibitors, such as phenprocoumon (compound **II**), provided a rational basis for the structure-based design of more active analogues. This investigation reports on the important finding of a carboxamide functionality appropriately added to the 4-hydroxycoumarin and the 4-hydroxy-2-pyrone templates which resulted in new promising series of nonpeptidic HIV protease inhibitors with improved enzyme-binding affinity. The most active diastereomer of the carboxamide-containing compound **XXIV** inhibited HIV-1 protease with a K_i value of $0.0014 \mu\text{M}$. This research provides a new design direction for the discovery of more potent HIV protease inhibitors as potential therapeutic agents for the treatment of HIV infection.

Introduction

The rapid spread of the acquired immunodeficiency syndrome (AIDS) epidemic has stimulated the discovery of therapeutic agents for arresting the replication of the causative virus, human immunodeficiency virus (HIV). One promising possibility for interrupting the viral life cycle is the use of inhibitors of the virally encoded protease which is indispensable for viral maturation.^{1,2} Among the most potent inhibitors reported thus far are peptidomimetic compounds containing transition-state inserts in place of the dipeptidic cleavage sites of the substrates.^{3–6} The low oral bioavailability and rapid biliary excretion of peptide-derived compounds⁷ have limited their utility as potential therapeutic agents. Recent advances have resulted in HIV protease inhibitors with reduced peptidic character and also nonpeptidic inhibitors that are more orally bioavailable, and an increasing number of HIV protease inhibitors^{8–20} are currently undergoing clinical evaluations.

We have previously reported on the potent peptidomimetic inhibitor U-75875 (1-(naphthoxyacetyl)-L-histidyl-5(S)-amino-6-cyclohexyl-3(R),4(R)-dihydroxy-2(R)-isopropylhexanoyl-L-isoleucine *N*-(2-pyridylmethyl)amide, compound **I** in Figure 1)^{21,22} which was shown to have an inhibitory effect on SIV in rhesus monkeys only after continuous intravenous infusion.²³ Interest in orally bioavailable HIV protease inhibitors led us to search for

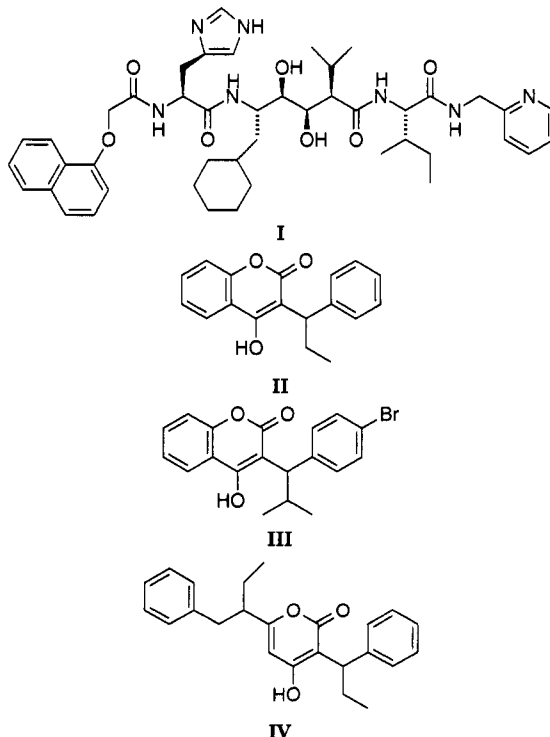


Figure 1. Structures of HIV protease inhibitors.

inhibitors in nonpeptidic templates that might offer superior biopharmaceutical properties. In a recent communication,²⁰ we reported on the identification of phenprocoumon (3-(α -ethylbenzyl)-4-hydroxycoumarin, compound **II** in Figure 1) from a broad screening program as a possible HIV protease inhibitory template. It is

[†] Medicinal Chemistry Research.

[‡] Physical & Analytical Chemistry.

[§] Computer-Aided Drug Discovery.

^{||} Chemical & Biological Screen.

[†] Cancer & Infectious Diseases Research.

[†] Molecular Biology.

[#] Biochemistry.

[§] Abstract published in *Advance ACS Abstracts*, August 1, 1995.

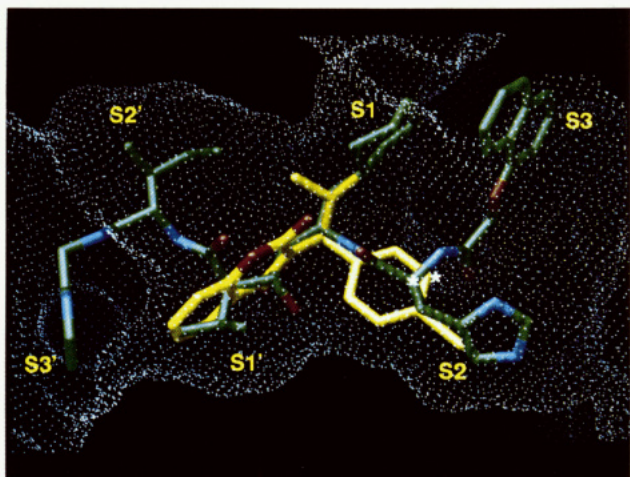


Figure 2. Overlay of compound **I** (primarily green) and compound **III** (primarily yellow) as found in the superimposed crystallographic structure determinations of the protease/inhibitor complexes, with nitrogens shown in blue and oxygens in red. The overlay shows the relative positioning of the two compounds in their HIV-1 protease-complexed positions. The white dot surface is a smoothed representation of the van der Waals surface of the HIV-1 protease binding site, as it appears in complex with compound **I**. The labels S_3 through S_3' approximately locate the six subsites³² commonly filled by peptidic inhibitors. The asterisks highlight the two atoms, one in each molecule, that led to the design strategy (described in the text) for improving the binding affinity of compounds in the series represented here by compound **III** (yellow).

noted that other independent studies^{24–28} have also described 4-hydroxybenzopyran-2-ones and 4-hydroxypyran-2-ones as inhibitors of HIV protease. An increasing number of reported crystal structures of inhibitor/HIV protease complexes have provided numerous successful examples of structure-based designs of potent HIV protease inhibitors.^{29,30} For our research program, the crystal structure of inhibitor **II**/HIV-1 protease complex formed the basis of iterative cycles of structure-based design of more active analogues. From that investigation, U-96988 (3-(α -ethylbenzyl)-6-(α -ethylphenethyl)-4-hydroxy-2*H*-pyran-2-one, compound **IV** in Figure 1) was identified as the first clinical candidate in this promising series of nonpeptidic HIV protease inhibitors as a potential therapeutic agent for the treatment of HIV infection.²⁰ The present report describes a structure-based design effort which relied on the information from the crystal structures of HIV protease complexes with a number of selected inhibitors. These findings resulted in the important identification of the carboxamide functionality in this series of inhibitors and pointed to an additional new direction of research that led to the preparation of inhibitors with higher binding affinity to HIV protease.

Initial Modeling Studies

As previously reported,²⁰ the X-ray crystallographic structure of compound **II** in a complex with HIV protease revealed a binding mode in which the 4-OH group interacted with the catalytic Asp25 and Asp25' residues of the enzyme, while the lactone oxygens of the inhibitor accepted additional hydrogen bonds from the Ile50 and Ile50' residues on the flaps of the enzyme which cover the catalytic cleft. We have also determined the crystal structure of compound **III** (yellow structure in Figure 2), which is the *p*-bromophenyl analogue of

compound **II** in the enzyme complex. The presence of the bromine atom and the higher resolution of the inhibitor **III**/enzyme complex led us to utilize this crystal structure for our initial modeling studies. As shown in Figure 2, an overlay of the X-ray crystal structures of the peptidic inhibitor **I**³¹ (in green) and compound **III** (in yellow) in their respective HIV protease-binding orientations pointed out a general correspondence of the two inhibitors in terms of their ability to reach the S_1' , S_1 , and S_2 pockets³² of the binding sites. It was also noted from this overlay that the close relative positioning of the histidine C α of the peptidic inhibitor **I** and the *meta* carbon of the phenyl ring in compound **III** (both positions are marked with white asterisks in Figure 2) suggested a strategy for designing substituents that would reach the S_3 pocket.

The portion of the structure of the peptidic inhibitor **I** (green structure in Figure 2) which extends from the histidine C α position and projects into the S_3 pocket of the enzyme contains a number of atoms which appear to form strong interactions with the protein. It was noted that the amide group attached to the C α forms two hydrogen bonds to the protein, one from its nitrogen to the Gly48 residue and the other from its carbonyl to the Asp29 residue. Furthermore, the naphthyl group at the end of the chain appears to form a hydrophobic interaction with the protein. From these observations, it was reasoned that attaching an amide-containing chain to the *meta* carbon of the phenyl ring of the smaller inhibitor, such as compound **II**, should direct the substituent along the same path seen in the peptidic inhibitor **I** and form the same hydrogen bonds. Termination of the chain with a bulky hydrophobic group should also, it was reasoned, fill the S_3 subsite, thereby improving the binding affinity of this series of inhibitors. This design strategy became the guide for a number of synthetic targets described below.

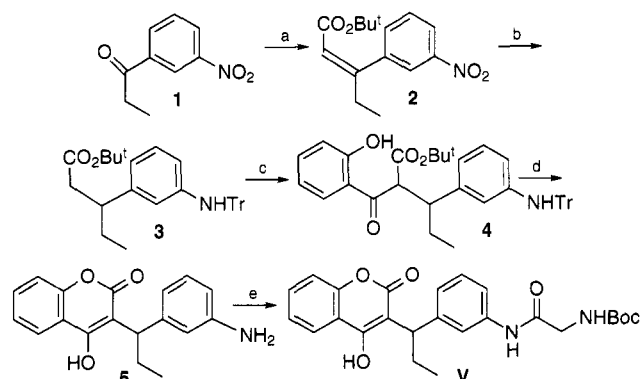
Chemistry

The preparation of compound **V**, which is a representative compound in Table 1, is shown in Scheme 1. *m*-Nitropropiophenone (**1**) was reacted with the anion of dimethyl [(*tert*-butyloxycarbonyl)methyl]phosphonate to give the α,β -unsaturated esters (**2**) as a mixture of *E* and *Z* isomers. The olefin and the nitro group were reduced by hydrogenation over platinum on carbon, and the resulting amino function was protected as the corresponding trityl group to give compound **3**. Deprotection with lithium diisopropylamide generated the ester enolate which was reacted with methyl salicylate to give the product **4**. Treatment with trifluoroacetic acid removed the *tert*-butyl ester protecting group and the trityl protecting group and further effected the 4-hydroxycoumarin ring closure to give the free amine **5**, which was utilized in the preparation of various HIV protease inhibitory analogues in this series. For example, the amine **5** was condensed with (*tert*-butyloxycarbonyl)glycine using diethyl cyanophosphonate to give the inhibitor **V**.

The preparation of compound **XVII**, which is a representative compound in Table 3, is shown in Scheme 2. 3-Propionylbenzonitrile (**6**) was reacted with the anion of dimethyl [(*tert*-butyloxycarbonyl)methyl]phosphonate to give the α,β -unsaturated esters as a mixture of *E* and *Z* isomers. This mixture was hydrogenated over palladium on carbon to give the corresponding

Table 1. HIV-1 Protease Inhibitory Activity of Carboxamide-Containing Phenprocoumons

compound	structure	K_i (μM)
V		0.16
VI		0.28
VII		1.6
VIII		0.17
IX		3.6
X		0.11

Scheme 1. Preparation of Compound **V**^a

^a (a) (H₃CO)₂P(O)CH₂CO₂Bu⁴, NaH; (b) H₂, Pt/C; (C₆H₅)₃CCl, Pr⁴N⁺Et⁻; (c) LiNPr⁴, methyl salicylate; (d) CF₃CO₂H; (e) Boc-gly, NCP(O)(OC₂H₅)₂.

saturated ester **7**. Basic hydrolysis of both the ester and the nitrile functional groups afforded the diacid intermediate which was subsequently protected as the *di-tert*-butyl ester **8** employing *N,N*-dimethylformamide *di-tert*-butyl acetal. Deprotonation with lithium diisopropylamide generated the ester enolate which was reacted with methyl salicylate to give the product **9**. Treatment with trifluoroacetic acid removed the *tert*-butyl ester protecting groups and effected ring closure to give the 4-hydroxycoumarin **10**, which was utilized in the preparation of various analogues in Table 3. For example, the carboxylic acid **10** was condensed with 1(*S*)-amino-2(*R*)-hydroxyindane using diethyl cyanophosphonate to give the inhibitor **XVII**.

The preparation of compound **XX**, which is a representative compound in Table 4, is shown in Scheme 3. Treatment of 4-hydroxy-6-methyl-2-pyrone (**11**) with 2 equiv of lithium diisopropylamide gave the corresponding dianion which could be alkylated at C-6 α with benzyl bromide to give 4-hydroxy-6-phenethyl-2-pyrone. The latter compound was then treated with 2 equiv of

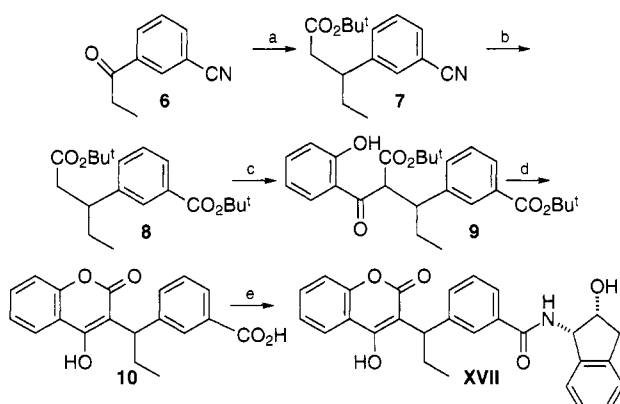
Table 2. HIV-1 Protease Inhibitory Activity of Carboxamide-Containing 4-Hydroxycoumarin Analogues

compound	structure	K_i (μM)
XI		0.56
XII		0.17
XIII		0.35
XIV		0.086
XV		0.17
XVI		0.028

Table 3. HIV-1 Protease Inhibitory Activity of Alternate Carboxamide-Containing Phenprocoumons

compound	structure	K_i (μM)
XVII		3.4
XVIII		4.4
XIX		0.4

lithium diisopropylamide to give the corresponding dianion which could be alkylated at C-6 α with ethyl iodide to give compound **12**. Nitration of cyclopropyl phenyl ketone (**13**) with fuming nitric acid gave predominantly the corresponding *m*-nitrophenyl ketone, which was reduced with gaseous hydrogen over platinum on carbon to give compound **14**. The amino function was protected as the corresponding benzyloxycarbonyl group by reaction with benzyl chloroformate and diisopropylethylamine. The ketone function was then reduced with sodium borohydride to give compound **15**. A *p*-toluenesulfonic acid-catalyzed condensation reaction between the 2-pyrone **12** and the benzylic alcohol **15** in benzene in the presence of molecular sieves provided the condensation product **16**. Hydrogenolysis of the benzyloxycarbonyl protecting group with ammonium formate over palladium on charcoal gave the

Scheme 2. Preparation of Compound **XVII**^a

^a (a) (H₃CO)₂P(O)CH₂CO₂Bu^t, NaH; H₂, Pd/C; (b) KOH, H₂O/EtOH; (CH₃)₂NCH[OC(CH₃)₃]₂; (c) LiNPr₂, methyl salicylate; (d) CF₃CO₂H; (e) 1(S)-amino-2(R)-hydroxyindane, NCP(O)(OC₂H₅)₂.

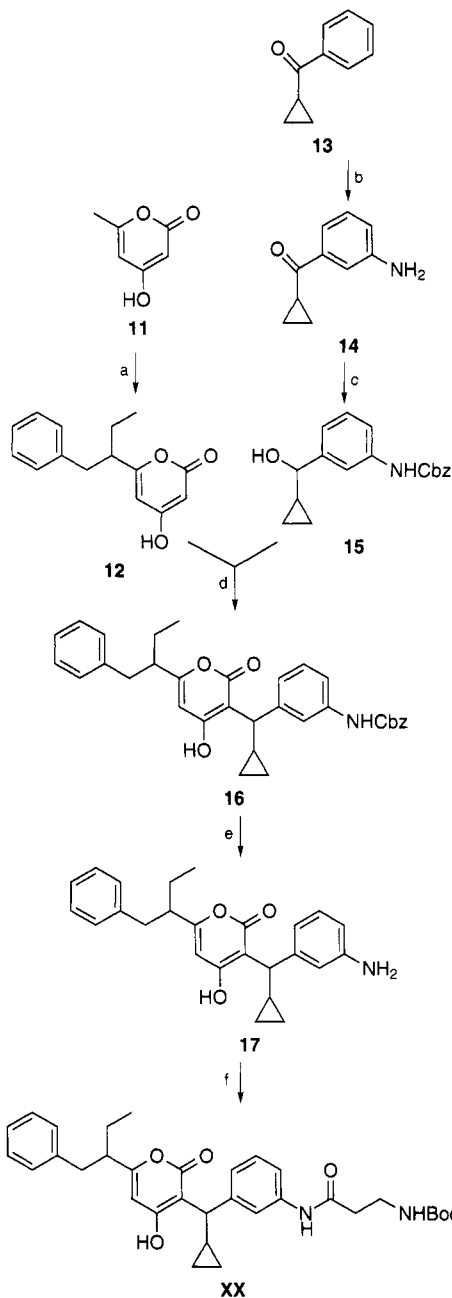
Table 4. HIV-1 Protease Inhibitory Activity of Carboxamide-Containing 4-Hydroxy-2-pyrone Analogues

compound	structure	K _i (μM)
XX		0.041
XXI		0.044
XXII		0.015
XXIII		0.019
XXIV		0.004

free amine 17, which was utilized in the preparation of various HIV protease inhibitory analogues in Table 4. For example, the amine 17 was condensed with (*tert*-butyloxycarbonyl)- β -alanine using diisopropylcarbodiimide to give the inhibitor **XX**.

Results and Discussion

The addition of a (*tert*-butyloxycarbonyl)glycyl residue to the *meta* amino functionality on the benzyl sidechain of phenprocoumon (compound **II**) provided the proposed inhibitor **V** (see Table 1). The notion that an inhibitor with a higher binding affinity could be realized is confirmed since compound **V** ($K_i = 0.16 \mu\text{M}$) showed significantly improved potency over the lead inhibitor

Scheme 3. Preparation of Compound **XX**^a

^a (a) 2 equiv of LiNPr₂, C₆H₅CH₂Br; 2 equiv of LiNPr₂, C₂H₅I; (b) HNO₃; H₂, Pt/C, CH₃OH; (c) C₆H₅CH₂O(CO)Cl, PrⁱNET; NaBH₄, EtOH; (d) TsOH, benzene; (e) (NH₄)(HCO₂), Pd/C, CH₃OH; (f) BocNHCH₂CH₂CO₂H, PrⁱN=C=NPⁱ.

II ($K_i = 1 \mu\text{M}$). It was therefore of interest to analyze with crystal structures whether this increased potency had, in fact, come about because of the improved interactions with the enzyme anticipated by the structure-based design strategy (*vide supra*). The crystal structure of compound **V** in HIV-2 protease complex was successfully obtained as shown in Figure 3 which illustrates the hydrogen-bonding interactions between the inhibitor and the enzyme, along with the amide functionality of the inhibitor **V** (in white) with the Gly48, Asp29, and Asp30 residues of the enzyme. First, since crystal structure determinations were performed with both the HIV-1 and HIV-2 proteases depending on the crystallographic quality of available crystals of any specific enzyme/inhibitor complexes, it was important to determine whether the binding of the inhibitors

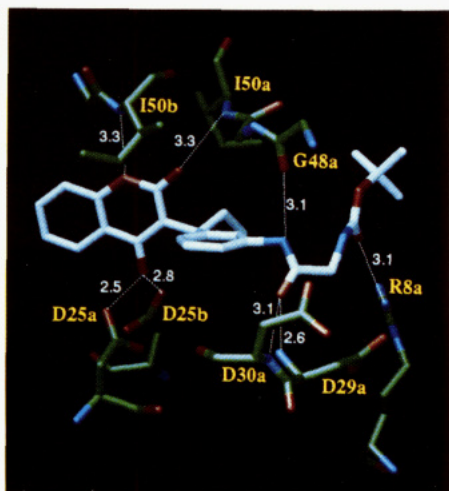


Figure 3. Interatomic distances of potential hydrogen-bonding atoms in the HIV-2 protease/V complex.

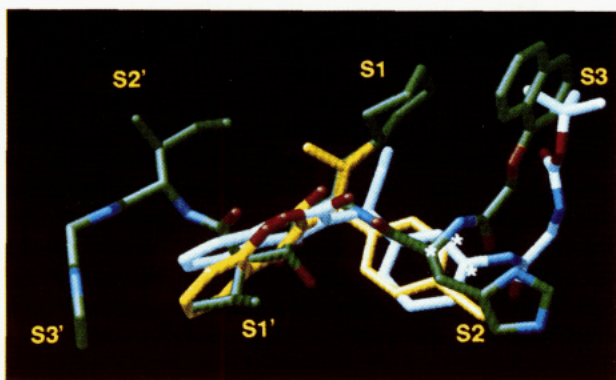


Figure 4. Overlay of compound V (primarily white) with those of compounds I and III (green and yellow, respectively, which were also shown in Figure 2) in their HIV protease-bound conformations. The three asterisks highlight the two atoms (as in Figure 2) that led to the *meta* attachment strategy, plus the corresponding *meta* position in the resulting compound V that was developed through this strategy. This overlay also illustrates the different paths followed by the green and white chains to reach the same S₃ subsite.

varies significantly with the source of the proteases. HIV-1 and HIV-2 proteases show 49% sequence homology, with homology being much higher in the inhibitor-binding regions. Nevertheless, some differences in the K_i values against the two enzymes are commonly found with many inhibitors, indicating that subtle differences exist. Second, due to the dimeric form of the HIV protease with the catalytic site intersecting the diad axis, most, but not all, of the crystallographic structure determinations result in two superimposed structures of the inhibitor in the binding site. This complicates the crystallographic structure determination but also indicates alternate ways to design inhibitors.

Figure 4 presents an overlay of the crystal structure of compound V (in white), in its bound conformation, with the two molecules (compound I in green and compound III in yellow) that were used to develop the strategy. Several interesting features can be seen in this overlay. First, attachment of the amide chain at the *meta* position of the phenyl ring did, in fact, place the terminal *tert*-butyloxycarbonyl group in the S₃ subsite of the enzyme, as intended. However, the path followed by the side chain to reach the S₃ pocket was somewhat different than had been expected (comparing

the white chain of compound V with the green chain of the peptidic inhibitor I). The *meta* amide carbonyl of compound V forms the same hydrogen bond to the Asp29 residue as was seen in the peptidic inhibitor I; however, its amide nitrogen is significantly displaced from the corresponding atom in inhibitor I. It can be seen in Figure 4 that this difference in amide locations can be accounted for by a slight rotation of the coumarin ring system around the C2 symmetry axis of the enzyme (comparing the white compound V with the yellow compound III). This in turn places the *meta* attachment atoms, highlighted with asterisks, in different positions, with a separation of 1.5 Å. It was assumed that the presence of the *p*-bromo group on the phenyl ring of the compound III (in yellow) played some role in this rotation effect. Overall, however, the original structure-based design hypothesis was validated by this analysis, and it led to further elaboration of *meta*-substituted analogues.

Further investigation of the possible addition of natural amino acids, containing the N-terminal *tert*-butyloxycarbonyl group, at the *meta* position of the phenyl ring was carried out with the automated *de novo* design program GROW.³³ The crystal structure of the complex of compound V (in white) with HIV protease (Figure 3) was used as a starting point. Removal of the (*tert*-butyloxycarbonyl)glycyl group from compound V resulted in a structure which was used as the growth seed for exploring potential ligand/enzyme interactions in the S₃ and S₄ regions. Growth was restricted to natural amino acids containing the N-terminal *tert*-butyloxycarbonyl group. The GROW program generated glycine, alanine, and proline in decreasing order of predicted preference and placed the *tert*-butyloxycarbonyl in the S₃ pocket in all three cases. When tested, the analogue with a (*tert*-butyloxycarbonyl)-L-alanyl residue (compound VIII) showed activity comparable to that of the inhibitor V, while the (*tert*-butyloxycarbonyl)-L-prolyl analogue (compound IX) was much less effective. In the non-natural amino acid cases, it was found that the corresponding (*tert*-butyloxycarbonyl)- β -alanyl analogue (compound VI) showed inhibitory activity comparable to that of the inhibitor V. However, the next homologue with the (*tert*-butyloxycarbonyl)- γ -aminobutyryl residue (compound VII) showed significantly reduced inhibitory activity. Finally, it should be noted that an equally effective inhibitor (compound X) with a non-amino acid residue could also be prepared. This latter compound provided a basis for possible further structure-activity study for this series of compounds which contain no amino acid residue.

In order to explore the possibility of improvement in inhibitory potency, additional analogues of compound VI were evaluated (see Table 2). It was noted from the crystal structure of inhibitor III (in yellow) in HIV protease complex (in Figure 2) that a substitution at the C-7 position on the coumarin ring might extend into an enzyme-binding pocket and would result in a compound with improved binding affinity. Compound XI was found to be more active ($K_i = 0.56 \mu\text{M}$) than the lead inhibitor II ($K_i = 1 \mu\text{M}$). Figure 5 shows the superposition of the two C₂ symmetric orientations (in white and yellow) of compound XI on the peptidic inhibitor I (in green) in HIV-2 protease complexes and confirmed the expected position of the 7-methoxy group

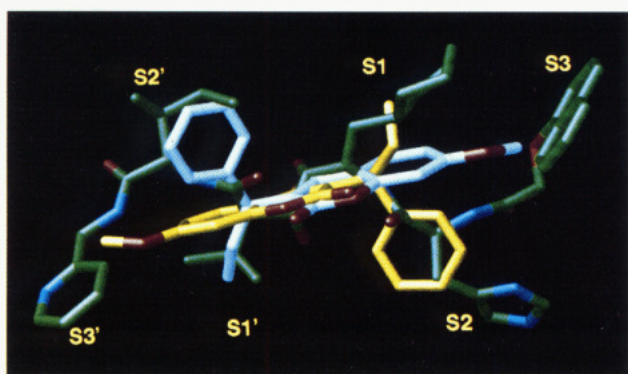


Figure 5. Overlay of the two compounds (**I** and **XI**) as found in the crystallographic structure determinations in HIV protease/inhibitor complexes. The least-squares fit of the protein molecules was used to superimpose the inhibitor molecules. The carbon atoms of compound **I** are colored green. While the protein dimer is located around a diad axis showing nearly 2-fold symmetry, the inhibitor is not symmetric and alternately occupies two orientations on the 2-fold axis. The two orientations of compound **XI** are shown with either yellow or white carbon atoms. The methoxy group extends toward the S_3 or S_3' subsites.

toward the S_3 binding pocket, bypassing the S_1 and S_2 pockets. Addition of the (*tert*-butyloxycarbonyl)- β -alanyl amino group to compound **XI** resulted then in the inhibitor **XII**, inhibitory activity of which was not significantly different from that of the inhibitor **VI**. On the basis of the crystal structure of the inhibitor **III**/HIV protease complex, a cyclopropyl group was evaluated at the C-3 α position in the inhibitor **II**. Compound **XIII** was shown to be more potent ($K_i = 0.35 \mu\text{M}$) than the lead inhibitor **II** ($K_i = 1 \mu\text{M}$). Addition of the (*tert*-butyloxycarbonyl)- β -alanyl amino group to compound **XIII** resulted in the inhibitor **XIV**, inhibitory activity of which was improved over that of the inhibitor **VI**. With both the 7-methoxy group and the C-3 α -cyclopropyl group, the inhibitor **XV** was significantly more active ($K_i = 0.17 \mu\text{M}$) than the lead inhibitor **II** ($K_i = 1 \mu\text{M}$). Addition of the (*tert*-butyloxycarbonyl)- β -alanyl amino group to compound **XV** resulted in the inhibitor **XIV** ($K_i = 28 \text{ nM}$) which exhibited 10-fold improvement in binding affinity over that of the inhibitor **VI**.

Due to the C_2 symmetric nature of the homodimeric HIV protease, the inhibitor **XI** could be found in the crystal structure of the HIV protease complex as having two orientations related by a 180° rotation (Figure 5). An overlay of the white structure of the inhibitor **XI** with that of the peptide-derived inhibitor **I** (in green) suggested a reversal of the amide functionality at the *meta* position of the benzyl side chain of the 4-hydroxycoumarin inhibitor; i.e. with the amide carbonyl attached to the phenyl ring rather than the amide nitrogen. A few potential inhibitors were then prepared on the basis of this observation (see Table 3). The amine residues for compound **XVII–XIX** were representatives of a few C-terminal functionality groups of many previously known peptide-derived HIV protease inhibitors. Smaller amine groups, such as those in compounds **XVII** and **XVIII**, resulted in inhibitors with relatively low potency. The L-isoleucyl 2-pyridylmethylamine group, as found in the peptide-derived inhibitor **I**, resulted in compound **XIX** with better inhibitory activity, although it showed less promise for additional structure–activity

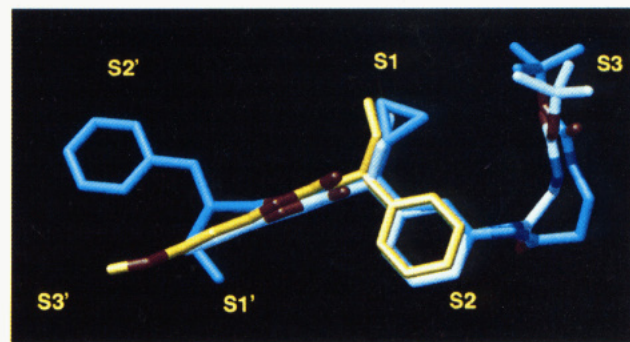


Figure 6. Overlay of three compounds as found in the superimposed crystallographic structure determinations. Carbons are colored white, yellow, and light blue for compounds **V**, **XI**, and **XX**, respectively. The additional methylene group of compound **XX** results in a wider arc and different protein interactions in reaching the S_3 subsite. The branched 6- α -groups fit better into the S_1' or S_2' subsites at the other end of the molecule.

study since it is larger in size and also relatively less active.

We have previously studied the 4-hydroxy-2-pyrone²⁰ as a different template derived from the 4-hydroxycoumarin analogues, and the inhibitor **IV** was reported as a clinical candidate. Using the corresponding C-3 α -cyclopropyl analogue of compound **IV**, carboxamides were added at the *meta* amino functionality of the benzyl side chain at C-3 and resulted in the compounds in Table 4. Addition of the (*tert*-butyloxycarbonyl)- β -alanyl residue gave the inhibitor **XX** with reasonably good inhibitory activity. The effect of the carboxamide functionality was more dramatic in the less coumarin series, since there is no improvement in binding affinity of compound **XX** as compared to the compound (analogue of compound **IV**) without the carboxamide functionality. The crystal structure of the inhibitor **XX** in the HIV-1 protease complex was then determined. Figure 6 shows the superposition of the inhibitors **V** (in white), **XI** (in yellow), and **XX** (in blue) in their respective crystal structure determinations. The pyrone rings along with the substituents in the S_1 and S_2 pockets overlay quite well. With the addition of an additional methylene group in compound **XX**, the region takes an even wider arc between the S_2 and S_3 pockets than did the inhibitor **V** and the carbonyl is rotated into the other direction. The (*tert*-butyloxycarbonyl) group occupies approximately the same position. At the C-6 substituent, the α -ethyl group fits better into the S_1' pocket than the coumarin does and the phenyl ring fits nicely into the S_2' pocket.

The corresponding (*tert*-butyloxycarbonyl)-L-alanyl analogue (compound **XXII**) showed improved potency. The inhibitor **XXIII**, with the large (*tert*-butyloxycarbonyl)- N^{im} -tosyl-L-histidyl group, exhibited no change in binding affinity as compared to the inhibitor **XXII**. The corresponding (*tert*-butyloxycarbonyl)-L-histidyl analogue (compound **XXIV**), however, showed further improvement in inhibitory potency ($K_i = 4 \text{ nM}$). In this particular case of compound **XXIV**, the four individual diastereomers were also prepared and shown to have K_i values of 1.4, 4.2, 6.3, and 8.5 nM, respectively. This observation would suggest that there is no highly significant impact on enzyme-binding affinity caused by the absolute stereochemistry at the two chiral centers. We have previously made similar observations with the

results for the four individual diastereomers of compound **IV**.²⁰ It should be noted that an effective inhibitor (compound **XXI**) with a non-amino acid residue could also be prepared. This latter compound also provided a basis for possible further structure–activity study for this series of compounds that contain no amino acid residue.

Compounds **XX–XXIV** were evaluated for antiviral activity in a cell culture assay. Cytotoxic effects in MT4 cells were evaluated using a modified MTT method.³⁴ All of these compounds were found to show no cytotoxic effect at 30 μM , and the CCTD₅₀ (cell culture toxicity dose₅₀) values were $>30 \mu\text{M}$. In MT4 cells acutely infected with HIV-1_{IIIB},³⁵ these compounds inhibited p24 production with IC₅₀ (inhibitory concentration₅₀) values in the range of 3–6 μM , which is comparable to that previously reported for the inhibitor **IV**.²⁰

Summary

From a broad screening program to discover nonpeptidic HIV protease inhibitors, phenprocoumon (compound **II**, $K_i = 1 \mu\text{M}$) was previously identified as a lead template. Overlay of the crystal structures of HIV protease complexes containing the peptide-derived inhibitor **I** and the nonpeptidic inhibitor **III** provided the basis for a molecular-modeling study that suggested the incorporation of a carboxamide functionality at the *meta* position of the benzyl side chain at C-3. Compound **V** was prepared and shown to have improved inhibitory activity over the reference compound **II**. A crystal structure of the inhibitor **V**/HIV protease complex was then determined, and the conformation of the inhibitor **V** in the enzyme active site was compared to that of the conformation expected from the modeling study. On the basis of this structure-based design of compound **V**, additional sets of analogues in the 4-hydroxycoumarin and the 4-hydroxy-2-pyrone series were prepared to evaluate the structure–activity relationship and to discover inhibitors with improved inhibitory potency. The inhibitor **XVI**, in the 4-hydroxycoumarin series, exhibited high HIV protease inhibitory activity with a K_i value of 28 nM. In the 4-hydroxy-2-pyrone series, the most active diastereomer of compound **XXIV** was found to show even higher inhibitory activity, with a K_i value of 1.4 nM. This finding of a specifically added carboxamide functionality to the inhibitory template, which resulted in inhibitors with improved enzyme-binding affinity, provides a new direction for the preparation of new promising series of potent and nonpeptidic HIV protease inhibitors. Although the compounds described in this report, such as the inhibitors **XVI** and **XXIV**, contain amino acid residues, compounds **X** and **XXI**, without amino acids, also showed high inhibitory activity. These latter two compounds provided a basis for the further exploration of more structure-based design experiments with non-amino acid-containing 4-hydroxycoumarin and 4-hydroxy-2-pyrone analogues which are expected to result in potent HIV protease inhibitors.

Experimental Section

Chemistry. Mass spectra, infrared spectra, and combustion analyses were obtained by the Physical and Analytical Chemistry Department of Upjohn Laboratories. ¹H NMR spectra were recorded at 300 MHz with a Bruker Model AM-300 spectrometer. Chemical shifts were reported as δ units

relative to tetramethylsilane as internal standard. Thin-layer chromatography was conducted with Analtech 0.25 mm glass plates precoated with silica gel GF. Chromatography used E. Merck silica gel 60 (70–230 mesh for column chromatography and 230–400 mesh for flash chromatography). All solvents for chromatography were reagent grade.

Reagents were from commercial sources and were used without further purification unless otherwise noted. Diethyl ether was Mallinkrodt anhydrous grade. Dichloromethane was dried over 4 Å molecular sieves. Diisopropylethylamine and benzene were distilled from calcium hydride. Diethyl cyanophosphonate was distilled before use. Tetrahydrofuran was distilled under argon from sodium metal in the presence of benzophenone.

(E)- and (Z)-3-(3-Nitrophenyl)pent-2-enoic Acid *tert*-Butyl Ester (2). Sodium hydride (1.0 g of 60% oil dispersion, 25 mmol) was suspended in 25 mL of benzene under argon in a flask immersed in an ice bath. To the stirred suspension was slowly added 4.8 mL (25 mmol) of *tert*-butyl (*P,P*-dimethylphosphono)acetate. The rate of addition was regulated to maintain the reaction temperature between 10 and 15 °C. Following the addition, the ice bath was removed and the mixture allowed to stir at room temperature for 60 min. After this time, 4.48 g (25 mmol) of finely powdered *m*-nitropropiophenone (**1**) was added as a solid. The reaction mixture was allowed to stir overnight. The resulting mixture was then partitioned between ether and aqueous NaHSO₄. The organic phase was washed with brine and dried (MgSO₄). The solvent was removed under reduced pressure and the residue flash chromatographed on silica gel 60 (230–400 mesh) with 10% ethyl acetate in hexane to afford 6.16 g (89%) of the mixture of (E)- and (Z)-3-(3-nitrophenyl)pent-2-enoic acid *tert*-butyl ester (**2**) as a yellow oil. The *E* and *Z* isomers were separable by column chromatography, although for the purpose of further synthesis, the mixture was utilized in the next chemical step. For isomer A: ¹H NMR (CDCl₃) δ 1.08 (t, $J = 7.5 \text{ Hz}$, 3H), 1.53 (s, 9H), 3.10 (q, $J = 7.5 \text{ Hz}$, 2H), 6.00 (s, 1H), 7.57 (t, $J = 8.0 \text{ Hz}$, 1H), 7.76 (m, 1H), 8.21 (m, 1H), 8.29 (m, 1H); TLC R_f 0.38 (15% ethyl acetate in hexane). For isomer B: ¹H NMR (CDCl₃) δ 1.07 (t, $J = 7.4 \text{ Hz}$, 3H), 1.24 (s, 9H), 2.46 (dq, $J = 7.4 \text{ Hz}$, $J = 1.5 \text{ Hz}$, 2H), 5.89 (m, 1H), 7.5 (m, 2H), 8.03 (m, 1H), 8.17 (m, 1H); TLC R_f 0.32 (15% ethyl acetate in hexane). For the *E* and *Z* mixture of unsaturated esters **2** as obtained from the reaction: EI MS *m/z* 277 (C₁₅H₁₉N₁O₄), 221 (C₁₁H₁₀N₁O₄), 204 (C₁₁H₁₀N₁O₃), 57 (C₄H₉); IR (thin film) 2977, 1712, 1531, 1349, 1150 cm⁻¹. Anal. (C₁₅H₁₉N₁O₄) C, H, N.

3-(3-Aminophenyl)pentanoic Acid *tert*-Butyl Ester. To a solution of 4.64 g (16.7 mmol) of the (E)- and (Z)-3-(3-nitrophenyl)pent-2-enoic acid *tert*-butyl ester (**2**) in 40 mL of methanol was added 260 mg of 5% platinum on carbon. The resulting mixture was placed in a Parr apparatus and shaken under 50 psi of H₂ gas overnight. The mixture was filtered through a pad of Celite with ethyl acetate rinses, and the filtrate was concentrated under reduced pressure to provide 4.15 g of 3-(3-aminophenyl)pentanoic acid *tert*-butyl ester as a tan oil: ¹H NMR (CDCl₃) δ 0.79 (t, $J = 7.4 \text{ Hz}$, 3H), 1.34 (s, 9H), 1.6 (m, 2H), 2.5 (2 dd, 2H), 2.85 (m, 1H), 3.6 (br, 2H), 6.5 (m, 3H), 7.1 (m, 1H); EI MS *m/z* 249 (C₁₅H₂₃N₁O₂), 193 (C₁₁H₁₄N₁O₂ + H₁), 176 (C₁₁H₁₄N₁O₁), 134 (C₉H₁₂N₁), 57 (C₄H₉).

3-[3-((Triphenylmethyl)amino)phenyl]pentanoic Acid *tert*-Butyl Ester (3). To a stirred solution of 4.15 g (16.6 mmol) of 3-(3-aminophenyl)pentanoic acid *tert*-butyl ester and 3.5 mL (20 mmol) of diisopropylethylamine in 40 mL of dichloromethane was added 5.10 g (18 mmol) of chlorotriphenylmethane in several portions over the course of about 10 min. The resulting solution was stirred at room temperature overnight. The solvent was then removed under reduced pressure and the residue partitioned between ethyl acetate and cold water. The aqueous phase was extracted with ethyl acetate and the combined organic phase washed with brine and then dried (MgSO₄). After removal of the solvent under reduced pressure, the residue was flash chromatographed on silica gel 60 (230–400 mesh), using 10% ethyl acetate in hexane as eluant, to provide 8.75 g of 3-[3-[(triphenylmethyl)amino]phenyl]pentanoic acid *tert*-butyl ester (**3**) as a white

solid: ^1H NMR (CDCl_3) δ 0.57 (t, $J = 7.3$ Hz, 3H), 1.3 (m, 2H), 1.36 (s, 9H), 2.24 (2 dd, 2H), 2.55 (m, 1H), 5.01 (br, 1H), 6.14 (m, 1H), 6.25 (dd, 1H), 6.40 (d, $J = 7.6$ Hz, 1H), 6.86 (t, $J = 7.8$ Hz, 1H), 7.2–7.4 (m, 15H); EI MS m/z 491 ($\text{C}_{34}\text{H}_{37}\text{N}_1\text{O}_2$), 243 ($\text{C}_{19}\text{H}_{15}$), 165 ($\text{C}_{13}\text{H}_{10}-\text{H}_1$); IR (thin film) 3418, 2958, 2925, 2856, 1729, 1602, 1485, 1446, 1153, 1145, 702, 698 cm^{-1} ; TLC R_f 0.32 (10% ethyl acetate in hexane). Anal. ($\text{C}_{34}\text{H}_{37}\text{N}_1\text{O}_2$) C, H, N.

3-[3-[(Triphenylmethyl)amino]phenyl]-2-(2-hydroxybenzoyl)pentanoic Acid *tert*-Butyl Ester (4). To 25 mL of dry tetrahydrofuran and 3.7 mL (26 mmol) of dry diisopropylamine under argon at -78°C was added 16.1 mL of a 1.6 M solution of butyllithium in hexane (25 mmol) over a few minutes. The solution was then warmed to 0°C , kept at this temperature for 10 min, and the re-cooled to -78°C . Into this stirred solution was slowly added a solution of 8.2 g (16.6 mmol) of 3-[3-[(triphenylmethyl)amino]phenyl]pentanoic acid *tert*-butyl ester (3) in 25 mL of dry tetrahydrofuran. The resulting solution was allowed to stir for 50 min at -78°C , giving a red-orange solution. To this stirred solution was added dropwise 1.1 mL (8.5 mmol) of methyl salicylate. After 5 min, the resulting solution was allowed to warm to ambient temperature. The mixture's color changed to very deep red and then lightened substantially overnight. The reaction mixture was partitioned between ethyl acetate and ice–water containing 100 mL of pH 7 phosphate buffer and 50 mL of 1 M aqueous KHSO_4 . The aqueous phase (near neutral pH) was extracted with ethyl acetate. The combined organic phase was dried (MgSO_4). Removal of the solvents under reduced pressure provided a crude mixture of the desired product and starting material. Flash chromatography of this mixture on silica gel (230–400 mesh) using 60–70% dichloromethane in hexane as eluant gave 4.87 g (94%) of 3-[3-[(triphenylmethyl)amino]phenyl]-2-(2-hydroxybenzoyl)pentanoic acid *tert*-butyl ester (4) as a tan foam: ^1H NMR (CDCl_3) δ 0.41 (t, $J = 7.2$ Hz, 3H), 1.13 (s, 9H), 3.19 (dt, 1H), 4.28 (d, $J = 11.0$ Hz, 1H), 6.25 (m, 2H), 4.48 (d, $J = 7.6$ Hz, 1H), 6.68–7.0 (m, 3H), 7.2–7.4 (m, 7.5 (m, 1H), 7.84 (dd, $J = 8.2$ Hz, $J = 1.6$ Hz, 1H); FAB MS [$\text{M} + \text{H}]^+$ m/z 612 ($\text{C}_{41}\text{H}_{41}\text{N}_1\text{O}_4$), 534 ($\text{C}_{35}\text{H}_{36}\text{N}_1\text{O}_4$), 434 ($\text{C}_{30}\text{H}_{27}\text{N}_1\text{O}_2 + \text{H}_1$), 243 ($\text{C}_{19}\text{H}_{15}$); TLC R_f 0.26 (65% dichloromethane in hexane). Anal. ($\text{C}_{41}\text{H}_{41}\text{N}_1\text{O}_4$) C, H, N.

3-[1-(3-Aminophenyl)propyl]-4-hydroxycoumarin (5). To 918 mg (1.50 mmol) of 3-[3-[(triphenylmethyl)amino]phenyl]-2-(2-hydroxybenzoyl)pentanoic acid *tert*-butyl ester (4) was added 6 mL of trifluoroacetic acid. The resulting solution was stirred at room temperature for 24 h. Trifluoroacetic acid was then removed under reduced pressure and the residue partitioned between dichloromethane and cold pH 7 phosphate buffer, and sufficient aqueous NaOH was added to render the aqueous phase neutral. The biphasic mixture, containing a small amount of undissolved solid, was placed in a continuous extractor and extracted overnight with a brisk flow of dichloromethane. The organic extract was then removed and dried (Na_2SO_4). Removal of the solvent under reduced pressure was followed by flash column chromatography on silica gel 60 (230–400 mesh). Elution with 50–100% ethyl acetate in hexane was followed by elution with 5% methanol in ethyl acetate. Product fractions were combined and concentrated to provide 369 mg (83%) of 3-[1-(3-aminophenyl)propyl]-4-hydroxycoumarin (5) as a tan solid: ^1H NMR (CDCl_3) δ 1.02 (t, $J = 7.3$ Hz, 3H), 2.12 (m, 2H), 4.41 (t, $J = 7.7$ Hz, 1H), 4.6 (br), 6.60 (dd, $J = 7.9$ Hz, $J = 2.3$ Hz, 1H), 6.75 (m, 1H), 6.88 (d, $J = 7.7$ Hz, 1H), 7.1–7.3 (m, 3H), 7.48 (m, 1H), 7.71 (dd, $J = 7.9$ Hz, $J = 1.6$ Hz, 1H); EI HRMS m/z 295.1213 (calcd for $\text{C}_{18}\text{H}_{17}\text{NO}_3$, 295.1208); TLC R_f 0.24 (30% ethyl acetate in dichloromethane).

4-Hydroxy-3-[1-[3-[[[(*tert*-butyloxycarbonyl)amino]methyl]carbonyl]amino]phenyl]propylcoumarin (V). To a cold (0°C) stirred solution of 22.2 mg (75 μmol) of 3-[1-(3-aminophenyl)propyl]-4-hydroxycoumarin (5) and 17 mg (97 μmol) of Boc-glycine in 0.5 mL of dichloromethane was added 17 μL (97 μmol) of diisopropylethylamine, followed by 14 μL (91 μmol) of diethyl cyanophosphonate. The ice bath was removed and the solution stirred overnight. Flash chromatography of the concentrated reaction mixture on silica gel, eluting with 60% ethyl acetate in dichloromethane and then

with 5, 10, and 15% methanol in this solvent, provided 21 mg (62%) of 4-hydroxy-3-[1-[3-[[[(*tert*-butyloxycarbonyl)amino]methyl]carbonyl]amino]phenyl]propylcoumarin (V) as an amorphous white solid: ^1H NMR ($\text{CDCl}_3 + \text{CD}_3\text{OD}$) δ 0.91 (t, $J = 7.3$ Hz, 3H), 1.43 (s, 9H), 2.1 (m, 1H), 2.3 (m, 1H), 3.8 (br, 2H), 4.3 (m, 1H), 7.2 (m, 5H), 7.4 (m, 1H), 7.6 (br, 1H), 7.87 (d, $J = 7.4$ Hz, 1H); EI HRMS m/z 452.1946 (calcd for $\text{C}_{25}\text{H}_{28}\text{N}_2\text{O}_6$, 452.1947); TLC R_f 0.25 (50% ethyl acetate in dichloromethane).

Compounds VI–X, XII, XIV, and XVI were prepared in a manner similar to that of the preparation of compound V; their physical data are summarized as follows.

4-Hydroxy-3-[1-[3-[[3-[(*tert*-butyloxycarbonyl)amino]1-oxopropyl]amino]phenyl]propylcoumarin (VI): ^1H NMR (CDCl_3) δ 0.96 (t, $J = 7.4$ Hz, 3H), 1.41 (s, 9H), 2.2 (m, 1H), 2.35 (m, 1H), 2.52 (t, $J = 6.3$ Hz, 2H), 3.39 (t, $J = 6.3$ Hz, 2H), 3.9 (br, 3H), 4.32 (dd, $J = 9.1$ Hz, $J = 6.7$ Hz, 1H), 7.2–7.4 (m, 5H), 7.5–7.6 (m, 2H), 7.9 (m, 1H); FAB HRMS [$\text{M} + \text{H}]^+$ m/z 467.2198 (calcd for $\text{C}_{26}\text{H}_{31}\text{N}_2\text{O}_6$, 467.2182); TLC R_f 0.32 (5% methanol in dichloromethane).

4-Hydroxy-3-[1-3-[[4-[(*tert*-butyloxycarbonyl)amino]1-oxobutyl]amino]phenyl]propylcoumarin (VII): ^1H NMR (CDCl_3) δ 0.94 (t, $J = 7.3$ Hz, 3H), 1.41 (s, 9H), 1.82 (m, 2H), 2.2 (m, 1H), 2.3 (m, 3H), 3.1 (br t, 2H), 4.1 (br, 3H), 4.33 (dd, $J = 8.9$ Hz, $J = 6.8$ Hz, 1H), 7.1–7.4 (m, 6H), 7.6 (br, 1H), 7.9 (br d, 1H); FAB HRMS [$\text{M} + \text{H}]^+$ m/z 481.2347 (calcd for $\text{C}_{27}\text{H}_{33}\text{N}_2\text{O}_6$, 481.2338); TLC R_f 0.30 (5% methanol in dichloromethane).

2-[[3-[1-(4-Hydroxy-2-oxo-2*H*-1-benzopyran-3-yl)propyl]amino]-1-methyl-2-oxoethyl]carbamic acid *tert*-butyl ester (VIII): ^1H NMR (CDCl_3) δ 0.91 (br t, 3H), 1.35 (m, 3H), 1.40 (s, 9H), 2.16 (m, 1H), 2.3 (m, 1H), 4.3 (m, 2H), 7.1–7.3 (m, 5H), 7.4 (m, 1H), 7.6 (br d, 1H), 7.9 (d, 1H); EI HRMS m/z 466.2099 (calcd for $\text{C}_{26}\text{H}_{30}\text{N}_2\text{O}_6$, 466.2104); TLC R_f 0.38 (50% ethyl acetate in dichloromethane).

2-[[3-[1-(4-Hydroxy-2-oxo-2*H*-1-benzopyran-3-yl)propyl]amino]carbonyl]-1-pyrrolidinecarboxylic acid *tert*-butyl ester (IX): ^1H NMR (CDCl_3) δ 0.9 (m, 3H), 1.1 (br, 4H), 1.25 (br, 9H), 1.9 (br, 2H), 2.2 (br, 3H), 3.5 (br, 2H), 4.5 (br, 1H), 7.0–7.3 (m, 4H), 7.5 (m, 2H), 8.0 (br, d, 1H), 9.9 (br, 1H); FAB HRMS [$\text{M} + \text{H}]^+$ m/z 493.2318 (calcd for $\text{C}_{28}\text{H}_{33}\text{N}_2\text{O}_6$, 493.2338); TLC R_f 0.31 (50% ethyl acetate in dichloromethane).

4-Hydroxy-3-[1-3-[[3-(1*H*-indol-1-yl)-1-oxopropyl]amino]phenyl]propylcoumarin (X): ^1H NMR (CDCl_3) δ 0.93 (t, $J = 7.3$ Hz, 3H), 2.15 (m, 1H), 2.3 (m, 1H), 2.75 (t, $J = 6.7$ Hz, 2H), 4.3 (m, 1H), 4.48 (t, $J = 6.7$ Hz, 2H), 6.41 (2s, 1H), 7.0–7.25 (m, 8H), 7.4 (m, 3H), 7.57 (d, $J = 7.8$ Hz, 1H), 7.88 (d, $J = 6.6$ Hz, 1H); EI HRMS m/z 466.1872 (calcd for $\text{C}_{29}\text{H}_{28}\text{N}_2\text{O}_4$, 466.1892); TLC R_f 0.37 (30% ethyl acetate in dichloromethane).

4-Hydroxy-3-[1-3-[[3-(1*H*-indol-1-yl)-1-oxopropyl]amino]phenyl]propyl-7-methoxycoumarin (XII): ^1H NMR (CDCl_3) δ 0.95 (t, $J = 7.3$ Hz, 3H), 1.42 (s, 9H), 2.2 (m, 1H), 2.3 (m, 1H), 2.52 (t, $J = 6.3$ Hz, 2H), 3.39 (t, $J = 6.3$ Hz, 2H), 3.84 (s, 3H), 4.0 (br, 3H), 4.28 (dd, $J = 9.1$ Hz, $J = 6.7$ Hz, 1H), 6.74 (d, $J = 2.4$ Hz, 1H), 6.83 (dd, $J = 8.9$ Hz, $J = 2.4$ Hz, 1H), 7.2 (m, 2H), 7.35 (m, 1H), 7.6 (br, 1H), 7.77 (d, $J = 8.9$ Hz, 1H); FAB HRMS [$\text{M} + \text{H}]^+$ m/z 497.2301 (calcd for $\text{C}_{27}\text{H}_{33}\text{N}_2\text{O}_7$, 497.2288); TLC R_f 0.29 (5% methanol in dichloromethane).

[3-[[3-Cyclopropyl(4-hydroxy-2-oxo-2*H*-1-benzopyran-3-yl)methyl]amino]-3-oxopropylcarbamic acid *tert*-butyl ester (XIV): ^1H NMR (CDCl_3) δ 0.33 (m, 2H), 0.52 (m, 1H), 0.78 (m, 1H), 1.41 (s, 9H), 1.9 (m, 1H), 2.51 (t, $J = 6.4$ Hz, 2H), 3.38 (t, $J = 6.4$ Hz, 2H), 3.62 (d, $J = 10$ Hz, 1H), 4.1 (br, 3H), 7.3–7.6 (m, 7H), 7.89 (dd, $J = 8.2$ Hz, $J = 1.5$ Hz, 1H); FAB HRMS [$\text{M} + \text{H}]^+$ m/z 479.2186 (calcd for $\text{C}_{27}\text{H}_{31}\text{N}_2\text{O}_6$, 479.2182); TLC R_f 0.28 (5% methanol in dichloromethane).

[3-[[3-Cyclopropyl(4-hydroxy-7-methoxy-2-oxo-2*H*-1-benzopyran-3-yl)methyl]amino]-3-oxopropylcarbamic acid *tert*-butyl ester (XVI): ^1H NMR (CDCl_3) δ 0.32 (m, 2H), 0.50 (m, 1H), 0.78 (m, 1H), 1.40 (s, 9H), 1.88 (m, 1H), 2.50 (t, $J = 6.3$ Hz, 2H), 3.37 (t, $J = 6.3$ Hz, 2H), 3.58 (d, $J = 10$ Hz, 1H), 3.84 (s, 3H), 4.0 (br, 3H), 6.76 (d, $J = 2.4$ Hz, 1H), 6.83 (dd, $J = 2.5$ Hz, $J = 8.9$ Hz, 1H), 7.2 (m, 2H), 7.4 (m, 1H), 7.6 (m, 1H), 7.77 (d, $J = 8.9$ Hz, 1H); FAB HRMS [$\text{M} + \text{H}]^+$

m/z 509.2282 (calcd for C₂₈H₃₈N₂O₇, 509.2288); TLC *R_f* 0.29 (5% methanol in dichloromethane).

3-(3-Cyanophenyl)pent-2-enoic Acid *tert*-Butyl Ester. To a suspension of 320 mg (60% dispersion in mineral oil, 8.0 mmol) of sodium hydride in 8.0 mL of dry benzene at 5 °C under argon was slowly added dropwise 1.45 mL (7.5 mmol) of dimethyl [(*tert*-butyloxycarbonyl)methyl]phosphonate. After 15 min, the solution was allowed to warm to room temperature. After 1.5 h, the solution was recooled to 5 °C and then treated with 1.06 g (6.67 mmol) of 3-propionylbenzonitrile (**6**) as a solid. The resulting mixture was allowed to warm to room temperature overnight. The reaction mixture was partitioned between diethyl ether and dilute aqueous KHSO₄. The aqueous layer was extracted with two additional portions of diethyl ether. The combined diethyl ether extractions were dried over MgSO₄, filtered, and finally concentrated under reduced pressure. The residue was purified by flash column chromatography on silica gel, eluting with 10% to 15% ethyl acetate in hexane to afford 1.71 g (6.65 mmol, 100%) of a mixture of diastereomers of 3-(3-cyanophenyl)pent-2-enoic acid *tert*-butyl ester as a clear colorless oil. Major diastereomer: ¹H NMR (CDCl₃) δ 7.7–7.6 (m, 3H), 7.52 (t, 1H, *J* = 7.8 Hz), 5.94 (s, 1H), 3.04 (q, 2H, *J* = 7.5 Hz), 1.53 (s, 9H), 1.06 (t, 3H, *J* = 7.5 Hz).

3-(3-Cyanophenyl)pentanoic Acid *tert*-Butyl Ester (7**).** To a Parr bottle containing 400 mg of 5% palladium on carbon was added 1.71 g (6.65 mmol) of the diastereomeric 3-(3-cyanophenyl)pent-2-enoic acid *tert*-butyl esters as a solution in 10 mL of ethyl acetate. The reaction mixture was shaken at 50 psi of hydrogen gas overnight. The resulting slurry was filtered through Celite with ethyl acetate washings. The combined filtrates were concentrated under reduced pressure to afford 1.60 g (6.18 mmol, 93%) of 3-(3-cyanophenyl)pentanoic acid *tert*-butyl ester (**7**) as a clear, colorless oil: ¹H NMR (CDCl₃) δ 7.55–7.35 (m, 4H), 3.0 (m, 1H), 2.60 (dd, 1H, *J* = 15 and 6.3 Hz), 2.45 (dd, 1H, *J* = 15 and 9.2 Hz), 1.8–1.5 (m, 2H), 1.30 (s, 9H), 0.80 (t, 3H, *J* = 7.4 Hz).

3-[1-(Carboxymethyl)propyl]benzoic Acid. To a stirred solution of 2.54 g (9.81 mmol) of 3-(3-cyanophenyl)pentanoic acid *tert*-butyl ester (**7**) in 5 mL of ethanol was added 15 mL of a 30% aqueous potassium hydroxide solution. The resulting mixture was heated at 70 °C overnight. The reaction mixture was then cooled to room temperature, diluted with water, and then washed with diethyl ether. The aqueous layer was acidified (pH = 2) with 6 N aqueous hydrochloric acid and repeatedly extracted with chloroform. The combined chloroform extractions were dried over MgSO₄, filtered, and finally concentrated under reduced pressure to afford 1.82 g (8.20 mmol, 84%) of 3-[1-(carboxymethyl)propyl]benzoic acid as a tan solid: ¹H NMR (CDCl₃) δ 12.1 (br s, 2H), 7.95 (m, 2H), 7.45 (m, 2H), 3.1 (m, 1H), 2.75 (dd, 1H, *J* = 16 and 6.7 Hz), 2.65 (dd, 1H, *J* = 16 and 8.4 Hz), 1.8–1.55 (m, 2H), 0.79 (t, 3H, *J* = 7.3 Hz); EI MS *m/z* 222 (M⁺), 204 (M⁺ – H₂O).

3-[1-(*tert*-Butoxycarbonyl)methyl]propyl]benzoic Acid *tert*-Butyl Ester (8**).** To a mixture of 0.22 g (1.0 mmol) of 3-[1-(carboxymethyl)propyl]benzoic acid in 10 mL of refluxing benzene under argon was added dropwise over 15 min 3.0 mL (11 mmol) of *N,N*-dimethylformamide di-*tert*-butyl acetal. After 2 h, the reaction mixture was cooled to room temperature and concentrated under reduced pressure. The residue was purified by flash column chromatography on silica gel, eluting with 10% ethyl acetate in hexanes to afford 0.25 g (0.75 mmol, 75%) of 3-[1-(*tert*-butoxycarbonyl)methyl]propyl]benzoic acid *tert*-butyl ester (**8**) as a clear colorless oil: ¹H NMR (CDCl₃) δ 7.83 (m, 2H), 7.84 (m, 2H), 3.0 (m, 1H), 2.59 (dd, 1H, *J* = 15 and 6.8 Hz), 2.47 (dd, 1H, *J* = 15 and 8.6 Hz), 1.8–1.5 (m, 2H), 1.60 (s, 9H), 1.30 (s, 9H), 0.79 (t, 3H, *J* = 7.4 Hz); MS (EI mode) *m/z* 278 (M⁺ – C₄H₈), 204 (M⁺ – C₈H₁₈O); ¹³C NMR (CDCl₃) δ 171.6, 165.9, 144.2, 132.0, 131.9, 128.7, 128.1, 127.5, 80.9, 80.2, 44.1, 42.5, 29.1, 28.2, 27.9, 11.9.

3-[2-(*tert*-Butoxycarbonyl)-1-ethyl-3-(2-hydroxyphenyl)-3-oxopropyl]benzoic Acid *tert*-Butyl Ester (9**).** To a solution of 0.38 mL (2.7 mmol) of diisopropylamine in 2.5 mL of dry tetrahydrofuran at –78 °C under argon was added 1.65 mL (2.64 mmol) of 1.6 M *n*-butyllithium in hexane. The solution was warmed to 0 °C for 20 min and then recooled to

–78 °C. The resulting solution was treated with 0.56 g (1.67 mmol) of 3-[1-[(*tert*-butoxycarbonyl)methyl]propyl]benzoic acid *tert*-butyl ester (**8**) as a solution in 2.5 mL of dry tetrahydrofuran. The resulting orange solution was stirred for 45 min and then treated with 0.11 mL (0.85 mmol) of methyl salicylate. The resulting reaction mixture was left to slowly warm to room temperature overnight. The reaction mixture was then concentrated under reduced pressure and partitioned between ethyl acetate and cold, dilute aqueous hydrochloric acid. The aqueous phase was extracted with additional portions of ethyl acetate. The combined ethyl acetate extractions were washed with brine, dried over MgSO₄, filtered, and finally concentrated under reduced pressure. The resulting residue was purified by flash column chromatography on silica gel, eluting with 10% to 25% ethyl acetate in hexane to afford 0.27 g (0.61 mmol, 71%) of diastereomeric 3-[2-(*tert*-butoxycarbonyl)-1-ethyl-3-(2-hydroxyphenyl)-3-oxopropyl]benzoic acid *tert*-butyl ester (**9**) as a pale oil. Major diastereomer: ¹H NMR (CDCl₃) δ 12.2 (s, 1H), 8.1–6.9 (m, 8H), 4.61 (d, 1H, *J* = 11 Hz), 3.60 (m, 1H), 1.8–1.4 (m, 2H), 1.62 (s, 9H), 1.04 (s, 9H), 0.71 (t, 3H, *J* = 7.3 Hz).

3-[1-(4-Hydroxy-2-oxo-2*H*-chromen-3-yl)propyl]benzoic Acid (10**).** To 276 mg (0.71 mmol) of 3-[2-(*tert*-butoxycarbonyl)-1-ethyl-3-(2-hydroxyphenyl)-3-oxopropyl]benzoic acid *tert*-butyl ester (**9**) was added 2 mL of trifluoroacetic acid. The resulting tan solution was left to stir at room temperature. After 14 h, the reaction mixture was concentrated under reduced pressure and the resulting residue triturated with toluene to remove the residual trifluoroacetic acid to afford 136 mg (0.42 mmol, 59%) of 3-[1-(4-hydroxy-2-oxo-2*H*-chromen-3-yl)propyl]benzoic acid (**10**) as a white solid: ¹H NMR (DMF-d₇) δ 8.15–7.35 (m, 8H), 4.56 (t, 1H), 2.41 (m, 1H), 2.26 (m, 1H), 0.96 (t, 1H, *J* = 7.3 Hz); EI MS *m/z* 324.0994 (calcd for C₁₉H₁₆O₅, 324.0998).

N-(2(R)-Hydroxyindan-1(S)-yl)-3-[1-(4-hydroxy-2-oxo-2*H*-1-benzopyran-3-yl)propyl]benzamide (XVII**).** To a stirred solution of 33 mg (102 μmol) of 3-[1-(4-hydroxy-2-oxo-2*H*-chromen-3-yl)propyl]benzoic acid (**10**) and 19 mg (127 μmol) of 1(S)-amino-2(R)-hydroxyindane³⁶ in 0.5 mL of dichloromethane was added 26 μL (149 μmol) of diisopropylethylamine, followed by 20 μL (132 μmol) of diethyl cyanophosphonate. The resulting solution was allowed to stir overnight. Flash chromatography of the concentrated reaction mixture on silica gel eluting with 2.5% to 10% methanol in dichloromethane provided 24 mg (53 μmol, 52%) of *N*-(2(R)-hydroxyindan-1(S)-yl)-3-[1-(4-hydroxy-2-oxo-2*H*-1-benzopyran-3-yl)propyl]benzamide (**XVII**) as an amorphous white solid: ¹H NMR (CDCl₃–CD₃OD) δ 8.0–7.1 (m, 12H), 5.10 (d, 1H, *J* = 5.0 Hz), 4.61 (m, 1H), 4.43 (t, 1H), 3.2–2.95 (m, 2H), 2.4 (m, 1H), 2.23 (m, 1H), 0.94 (t, 1H, *J* = 7.3 Hz); EI MS *m/z* 455.1741 (calcd for C₂₈H₂₅NO₅, 455.1733).

Compounds **XVIII** and **XIX** were prepared in a manner similar to that of the preparation of compound **XVII**; their physical data are summarized as follows.

3-[1-[[2-Benzimidazolyl)methyl]amino]carbonyl-phenyl]propyl]-4-hydroxycoumarin (XVIII**):** ¹H NMR (CDCl₃–CD₃OD) δ 8.0–7.2 (m, 12H), 4.79 (br s, 2H), 4.38 (t, 1H), 2.4–2.0 (m, 2H), 0.92 (t, 1H, *J* = 7.2 Hz); FAB MS *m/z* 454.1758 (calcd for C₂₇H₂₄N₃O₄, 454.1767).

3-[1-(4-Hydroxy-2-oxo-2*H*-1-benzopyran-3-yl)propyl]-N-[2-methyl-1-[[2-pyridinylmethyl]amino]carbonyl]-butyl]benzamide (XIX**):** ¹H NMR (CDCl₃–CD₃OD) δ 8.45 (m, 1H), 8.0–7.15 (m, 11H), 4.6–4.3 (m, 4H), 2.5–0.8 (m, 14H); FAB MS *m/z* 528.2506 (calcd for C₃₁H₃₄N₃O₅, 528.2498).

4-Hydroxy-6-phenethyl-2*H*-pyran-2-one. To a stirred solution of 0.90 mL (6.42 mmol) of diisopropylamine in 6 mL of anhydrous tetrahydrofuran at –78 °C under argon was added 4.0 mL (6.4 mmol) of a 1.6 M solution of *n*-butyllithium in hexane. The resulting solution was allowed to warm to 0 °C for 20 min and then treated with a solution of 378 mg (3.00 mmol) of 4-hydroxy-6-methyl-2-pyrone (**11**) in 17 mL of tetrahydrofuran. The resulting red, thick slurry was slowly treated with 6.0 mL of hexamethylphosphoramide and allowed to stir for 30 min. The resulting mixture was treated with 0.36 mL (3.03 mmol) of benzyl bromide. The resulting orange solution was allowed to stir at 0 °C for an additional 60 min.

The mixture was treated with excess 1 N aqueous hydrochloric acid, and the resulting yellow, biphasic mixture was concentrated to remove tetrahydrofuran. The remaining mixture was partitioned between dichloromethane and water, and the acidic aqueous phase was further extracted with additional portions of dichloromethane. The combined organic phase was dried over $MgSO_4$, and then concentrated under reduced pressure. The resulting residue was dissolved in diethyl ether and washed with dilute aqueous hydrochloric acid to remove most of the hexamethylphosphoramide. The ethereal phase was washed with brine, dried over $MgSO_4$, filtered, and finally concentrated under reduced pressure. The residue was flash column chromatographed on silica gel, eluting with 20% to 40% ethyl acetate in dichloromethane containing 1% acetic acid, to give 440 mg (2.04 mmol, 68%) of 4-hydroxy-6-phenethyl-2*H*-pyran-2-one as a tan solid: 1H NMR ($CDCl_3$ – CD_3OD) δ 7.35–7.05 (m, 5H), 5.85 (s, 1H), 5.46 (s, 1H), 2.95 (m, 2H), 2.76 (m, 2H); TLC R_f 0.38 (1% acetic acid and 25% ethyl acetate in dichloromethane); mp 137–138 °C (lit.³⁷ mp 137.5–138.5 °C).

6-(α -Ethylphenethyl)-4-hydroxy-2*H*-pyran-2-one (12). To a –78 °C stirred solution of 0.29 mL (2.1 mmol) of diisopropylamine in 4 mL of dry tetrahydrofuran, under argon, was added 1.2 mL of a 1.6 M solution (1.9 mmol) of *n*-butyllithium in hexane. The solution was warmed to 0 °C, kept at that temperature for 10 min, and then cooled to –30 °C. Into this solution of lithium diisopropylamide was cannulated a solution of 189 mg (0.874 mmol) of 4-hydroxy-6-phenethyl-2*H*-pyran-2-one in 4 mL of tetrahydrofuran. The resulting heterogeneous mixture was warmed to 0 °C, and sufficient hexamethylphosphoramide (ca. 1 mL) was added to render the mixture homogeneous. After the mixture was stirred for 30 min at 0 °C, 77 μ L (0.96 mmol) of ethyl iodide was added dropwise. After another 90 min, the reaction was quenched with excess 1 N HCl, and tetrahydrofuran was removed under reduced pressure. The residue was extracted with three portions of ethyl acetate and the combined organic extract washed with dilute HCl, dried ($MgSO_4$), and concentrated under reduced pressure. Flash chromatography of the residue on silica gel using 1% acetic acid and 25% ethyl acetate in dichloromethane provided 182 mg (85%) of the title compound: TLC R_f 0.33 (1% acetic acid and 25% ethyl acetate in dichloromethane); 1H NMR δ 0.85 (t, J = 7.4 Hz, 3H), 1.6 (m, 2H), 2.6 (m, 1H), 2.8 (m, 2H), 5.59 (s, 1H), 5.86 (s, 1H), 7.0–7.3 (m, 6H); FAB HRMS [M + H]⁺ m/z 245.1185 (calcd for $C_{15}H_{17}O_3$, 245.1178).

Cyclopropyl *m*-Nitrophenyl Ketone. To 130 mL of stirred fuming 90% nitric acid at –10 °C was added dropwise 21 mL (150 mmol) of cyclopropyl phenyl ketone (13). The rate of addition was regulated to maintain the reaction temperature at about –10 °C. Upon completion of addition, the resulting clear yellow solution was stirred for another 10 min at –10 °C and then poured into 1 L of crushed ice. The precipitated solid was extracted with 700 mL of toluene, and the organic extract was washed twice with 5% sodium hydroxide solution and once with brine and then dried over $MgSO_4$. The solvent was removed under reduced pressure, and the residue was recrystallized from methanol at –25 °C to give 14.6 g (50%) of cyclopropyl *m*-nitrophenyl ketone as dense, pale yellow prisms: 1H NMR ($CDCl_3$) δ 1.2 (m, 2H), 1.3 (m, 2H), 2.72 (tt, J_{cis} = 7.8 Hz, J_{trans} = 4.5 Hz, 1H), 7.70 (t, J = 8.0 Hz, 1H), 8.33 (d, J = 7.8 Hz, 1H), 8.43 (dd, J = 8.2 Hz, J = 2.3 Hz, 1H), 8.85 (m, 1H); IR (thin film) 1664, 1529, 1352, 1225, 1082, 1017, 852, 689 cm^{–1}; EI MS m/z 191; TLC R_f 0.32 (25% ethyl acetate in hexane); mp 71–73 °C. Anal. ($C_{10}H_9N_1O_3$) C, H, N. The mother liquor from the recrystallization contained mostly the corresponding *ortho* isomer.

***m*-Aminophenyl Cyclopropyl Ketone (14).** A solution of 5.76 g (30 mmol) of cyclopropyl *m*-nitrophenyl ketone in 100 mL of methanol was prepared with the aid of gentle heating. To this solution was added 450 mg of 5% platinum on carbon, and the resulting mixture was stirred vigorously under 1 atm of gaseous hydrogen. After 5 h, the mixture was filtered through a pad of Celite and the filtrate concentrated under reduced pressure to afford 4.89 g (100%) of *m*-aminophenyl cyclopropyl ketone (14) as an oil, which was carried on without further purification: 1H NMR ($CDCl_3$) δ 1.0 (m, 2H), 1.2, 2.6

(m, 2H), 3.9 (m, 1H), 6.85 (dd, J = 7.2 Hz, J = 2.5 Hz, 1H), 7.2 (m, 2H), 7.4 (m, 1H); TLC R_f 0.50 (80% ethyl acetate in hexane).

***m*-(Benzoyloxycarbonyl)amino]phenyl Cyclopropyl Ketone.** To a 0 °C, stirred solution of 4.89 g (30 mmol) of *m*-aminophenyl cyclopropyl ketone (14) and 6.3 mL (36 mmol) of diisopropylethylamine in 90 mL of dichloromethane was added dropwise 4.7 mL (33 mmol) of benzyl chloroformate. The resulting solution was allowed to warm to room temperature. After 4 h, the reaction mixture was washed with dilute hydrochloric acid and the aqueous phase extracted with two additional portions of dichloromethane. The combined organic phase was dried over $MgSO_4$ and then concentrated under reduced pressure to a yellow solid. This was triturated with two 30 mL portions of hexane, and the remaining solid was dried under reduced pressure to afford 8.74 g (98%) of *m*-(benzoyloxycarbonyl)amino]phenyl cyclopropyl ketone: 1H NMR δ 1.0–1.1 (m, 2H), 1.2–1.3 (m, 2H), 2.68 (m, 1H), 3.79 (s, 1H), 5.21 (s, 2H), 7.3–7.4 (m, 6H), 7.7 (m, 1H), 7.75 (br, 1H), 8.00 (m, 1H); IR 3305, 2925, 1728, 1655, 1549, 1216, 1069 cm^{–1}; EI MS m/z 295 ($C_{18}H_{17}NO_3$), 251 ($C_{10}H_{10}NO$ + C_7H_7). An analytical sample was recrystallized from methanol: mp 159–161 °C; TLC R_f 0.45 (5% ethyl acetate in dichloromethane). Anal. ($C_{18}H_{17}NO_3$) C, H, N.

***m*-(Benzoyloxycarbonyl)amino]phenyl Cyclopropyl Carbinol (15).** To a stirred solution of 8.74 g (29.6 mmol) of *m*-(benzoyloxycarbonyl)amino]phenyl cyclopropyl ketone in 100 mL of tetrahydrofuran and 100 mL of ethanol was added, in portions, 4.5 g (120 mmol) of sodium borohydride. After 3 h at room temperature, the reaction mixture was cooled in an ice bath while 100 mL of 1 N hydrochloric acid was slowly added. The resulting mixture was extracted with dichloromethane and the combined extract dried over $MgSO_4$. Solvent was removed under reduced pressure and the residue flash chromatographed on silica gel 60 (230–400 mesh) using 40% ethyl acetate in hexane to provide 8.48 g (96%) of *m*-(benzoyloxycarbonyl)amino]phenyl cyclopropyl carbinol (15) as a white crystalline solid: mp 91–92 °C; 1H NMR ($CDCl_3$) δ 0.3–0.6 (m, 4H), 1.1 (m, 1H), 2.35 (s, 1H), 3.92 (d, J = 8.3 Hz, 1H), 5.17 (s, 2H), 7.1 (m, 1H), 7.25 (t, J = 7.7 Hz, 1H), 7.3–7.5 (m, 7H); IR (thin film) 1693, 1599, 1559, 1449, 1235, 1054, 697 cm^{–1}; EI MS m/z 297; TLC R_f 0.28 (40% ethyl acetate in hexane). Anal. ($C_{18}H_{19}N_1O_3$) C, H, N.

3[α -Cyclopropyl-*m*-(benzoyloxycarbonyl)amino]benzyl]-6-(α -ethylphenethyl)-4-hydroxy-2*H*-pyran-2-one (16). A mixture of 2.01 g (8.2 mmol) of 6-(α -ethylphenethyl)-4-hydroxy-2*H*-pyran-2-one (12), 2.45 g (8.2 mmol) of *m*-(benzoyloxycarbonyl)amino]phenyl cyclopropyl carbinol (15), and 300 mg (1.6 mmol) of *p*-toluenesulfonic acid monohydrate in 16 mL of benzene was refluxed under argon for 21 h. The mixture was cooled and then concentrated under reduced pressure, and the resulting residue was flash chromatographed on silica gel 60 (230–400 mesh) using 5, 10, and 20% ethyl acetate in dichloromethane to provide 2.43 g (56%) of 3-[α -cyclopropyl-*m*-(benzoyloxycarbonyl)amino]benzyl]-6-(α -ethylphenethyl)-4-hydroxy-2*H*-pyran-2-one (16): 1H NMR ($CDCl_3$) δ 0.26 (m, 2H), 0.46 (m, 1H), 0.66 (m, 1H), 0.78 (2t, J = 7.4 Hz, 3H), 1.6 (m, 2H), 1.8 (m, 1H), 2.4 (m, 1H), 2.7 (m, 1H), 2.9 (m, 1H), 3.45 (d, J = 9.9 Hz, 1H), 5.12 (s, 2H), 5.85 (s, 1H), 6.79 (br, 1H), 6.9–7.4 (m, 14H), 9.56 (br, 1H); EI HRMS m/z 523.2350 (calcd for $C_{33}H_{33}NO_5$; 523.2359); TLC R_f 0.27 (5% ethyl acetate in dichloromethane).

3-(α -Cyclopropyl-*m*-aminobenzyl)-6-(α -ethylphenethyl)-4-hydroxy-2*H*-pyran-2-one (17). A mixture of 2.43 g (4.64 mmol) of 3-[α -cyclopropyl-*m*-(benzoyloxycarbonyl)amino]benzyl]-6-(α -ethylphenethyl)-4-hydroxy-2*H*-pyran-2-one (16), 2.93 g (46 mmol) of ammonium formate, and 250 mg of 5% palladium on carbon in 20 mL of methanol was stirred under argon for 1.5 h. An additional 250 mg of catalyst was added and stirring continued for an additional 1 h, at which time TLC indicated completion of the reaction. The mixture was filtered through Celite and the filtrate concentrated under reduced pressure. Following trituration with dichloromethane to separate the product from ammonium salts, the crude amine was flash chromatographed on silica gel 60 (230–400 mesh)

using 35–50% ethyl acetate in dichloromethane to give 1.65 g (91%) of 3-(α -cyclopropyl- m -aminobenzyl)-6-(α -ethylphenethyl)-4-hydroxy-2H-pyran-2-one (**17**): ^1H NMR (CDCl_3) δ 0.3 (m, 2H), 0.5 (m, 1H), 0.65 (m, 1H), 0.81 (2t, J = 7.3 Hz, 3H), 1.6 (m, 3H), 2.5 (m, 1H), 2.7 (m, 1H), 2.9 (m, 1H), 3.46 (2d, J = 9.8 Hz, 1H), 5.81 (2s, 1H), 6.49 (d, J = 7.9 Hz, 1H), 6.80 (s, 1H), 6.9–7.3 (m, 7H); TLC R_f 0.38 (30% ethyl acetate in dichloromethane); EI MS m/z 389, 361 ($\text{C}_{24}\text{H}_{27}\text{NO}_2$), 360 ($\text{C}_{23}\text{H}_{22}\text{NO}_3$).

[3-[3-Cyclopropyl[4-hydroxy-2-oxo-6-[1-(phenylmethyl)propyl]-2H-pyran-3-yl]methyl]phenyl]amino]-3-oxopropyl]carbamic acid tert-butyl Ester (XX**).** To a stirred solution of 50 mg (0.13 mmol) of 3-(α -cyclopropyl- m -aminobenzyl)-6-(α -ethylphenethyl)-4-hydroxy-2H-pyran-2-one (**17**) and 29 mg (0.15 mmol) of (*tert*-butyloxycarbonyl)- β -alanine in 0.5 mL of dichloromethane was added 22 μL (0.14 mmol) of diisopropylecarbodiimide. The resulting solution was stirred for 18 h and then flash chromatographed on silica gel 60 (230–400 mesh) using 5–10% methanol and 30% ethyl acetate in dichloromethane. The resulting material, slightly contaminated with diisopropylurea, was rechromatographed on silica using 30–70% ethyl acetate in dichloromethane, affording 34 mg (47%) of [3-[3-[cyclopropyl[4-hydroxy-2-oxo-6-[1-(phenylmethyl)propyl]-2H-pyran-3-yl]methyl]phenyl]amino]-3-oxopropyl]carbamic acid *tert*-butyl ester (**XX**) as a white solid: ^1H NMR (CDCl_3) δ 0.2 (m, 2H), 0.5 (m, 1H), 0.6 (m, 1H), 0.81 (2t, J = 7.4 Hz, 3H), 1.41 (s, 9H), 1.6 (m, 2H), 1.8 (m, 1H), 2.4 (m, 3H), 2.8 (m, 1H), 2.9 (m, 1H), 3.3 (m, 2H), 3.4 (m, 1H), 5.4 (m, 1H), 5.85 (2s, 1H), 7.0–7.3 (m, 7H), 7.5 (m, 2H); FAB HRMS [$M + \text{H}]^+$ m/z 561.2995 (calcd for $\text{C}_{33}\text{H}_{41}\text{N}_2\text{O}_6$, 561.2964); TLC R_f 0.17 (30% ethyl acetate in dichloromethane).

Compounds **XXI**–**XXIV** were prepared in a manner similar to that of the preparation of compound **XX**; their physical data are summarized as follows.

N-[3-Cyclopropyl[4-hydroxy-2-oxo-6-[1-(phenylmethyl)propyl]-2H-pyran-3-yl]methyl]phenyl]-4-pyridylacetamide (XXI**):** ^1H NMR (CDCl_3) δ 0.22 (m, 2H), 0.48 (m, 1H), 0.64 (m, 1H), 0.82 (m, 3H), 1.6 (m, 2H), 1.9 (m, 1H), 2.5 (m, 1H), 2.8 (m, 1H), 2.9 (m, 1H), 3.3 (m, 1H), 5.71 (2s, 1H), 7.0 (m, 2H), 7.2 (m, 5H), 7.3 (m, 2H), 7.5 (m, 2H), 8.4 (m, 2H); IR (thin film) 1673, 1607, 1414, 1288, 732 cm^{-1} ; EI HRMS m/z 508.2356 (calcd for $\text{C}_{32}\text{H}_{32}\text{N}_2\text{O}_4$, 508.2362); TLC R_f 0.30 (8% methanol in dichloromethane).

[3-[3-Cyclopropyl[4-hydroxy-2-oxo-6-[1-(phenylmethyl)propyl]-2H-pyran-3-yl]methyl]phenyl]amino]-2-methyl-3-oxopropyl]carbamic acid *tert*-butyl ester (XXII**):** ^1H NMR (CDCl_3) δ 0.2 (m, 2H), 0.4 (m, 1H), 0.6 (m, 1H), 0.8 (m, 3H), 1.4 (br t, 3H), 1.42 (s, 9H), 1.7 (m, 3H), 2.5 (m, 1H), 2.7 (m, 1H), 2.9 (m, 1H), 3.4 (m, 1H), 4.3 (br, 1H), 5.5 (br, 1H), 5.8 (br, 1H), 7.0–7.5 (m, 8H), 7.6 (m, 1H), 8.75 (br, 1H); IR 1672, 1562, 1415, 1165, 733 cm^{-1} ; FAB HRMS [$M + \text{Na}]^+$ m/z 583.2801 (calcd for $\text{C}_{33}\text{H}_{40}\text{N}_2\text{O}_8\text{Na}$, 583.2784); TLC R_f 0.35 (2% acetic acid and 20% ethyl acetate in dichloromethane).

[3-[3-Cyclopropyl[4-hydroxy-2-oxo-6-[1-(phenylmethyl)propyl]-2H-pyran-3-yl]methyl]phenyl]amino]-2-[1-(4-methylbenzenesulfonyl)imidazol-4-yl]-2-methyl-3-oxopropyl]carbamic acid *tert*-butyl ester (XXIII**):** ^1H NMR (CDCl_3) δ 0.1 (br, 1H), 0.2 (br, 1H), 0.5 (Br, 1H), 0.5 (br, 2H), 0.75 (m, 3H), 1.35 (s, 9H), 1.6 (m, 2H), 1.8 (br, 1H), 2.35 (s, 3H), 2.5 (m, 1H), 2.7 (m, 1H), 2.9 (m, 3H), 3.35 (m, 1H), 4.6 (br, 1H), 5.77 (s, 1H), 6.1 (m, 1H), 7.0–8.0 (m, 16H), 9.03 (br, 1H); IR (thin film) 1673, 1414, 1383, 1174, 1093, 733, 675 cm^{-1} ; FAB HRMS [$M + \text{H}]^+$ m/z 781.3268 (calcd for $\text{C}_{43}\text{H}_{48}\text{N}_4\text{O}_8\text{S}_1$, 781.3271); TLC R_f 0.26 (2% acetic acid and 20% ethyl acetate in dichloromethane).

[3-[3-Cyclopropyl[4-hydroxy-2-oxo-6-[1-(phenylmethyl)propyl]-2H-pyran-3-yl]methyl]phenyl]amino]-1(S)-[(1H-imidazol-4-yl)methyl]-2-oxoethyl]carbamic acid *tert*-butyl ester (XXIV**):** ^1H NMR (CDCl_3) δ 0.23 (m, 2H), 0.5 (m, 1H), 0.7 (m, 1H), 0.85 (m, 3H), 1.37 (2s, 9H), 1.6 (m, 2H), 1.9 (br, 1H), 2.5 (m, 1H), 2.8 (m, 1H), 3.0 (m, 3H), 3.35 (m, 1H), 4.5 (m, 1H), 5.75 (2s, 1H), 6.7 (m, 1H), 7.0–7.5 (m, 10H); IR 1664, 1490, 1410, 1166, 733 cm^{-1} ; FAB HRMS [$M + \text{H}]^+$ m/z 627.3186 (calcd for $\text{C}_{36}\text{H}_{43}\text{N}_4\text{O}_6$, 627.3182); TLC R_f 0.44 (15% methanol in dichloromethane).

The four individual diastereomers of compound **XXIV** were obtained via chiral HPLC preparative work; their physical data are summarized as follows.

[3-[(3(R)- or [3-[(3(S)-[Cyclopropyl[4-hydroxy-2-oxo-6-[1(R)-(phenylmethyl)propyl]-2H-pyran-3-yl]methyl]phenyl]amino]-1(S)-[(1H-imidazol-4-yl)methyl]-2-oxoethyl]carbamic acid *tert*-butyl ester (isomer 1 of **XXIV):** ^1H NMR (CDCl_3) δ 0.23 (m, 2H), 0.48 (m, 1H), 0.68 (m, 1H), 0.85 (t, J = 7.3 Hz, 3H), 1.38 (s, 9H), 1.6 (m, 2H), 1.9 (m, 1H), 2.5 (m, 1H), 2.8 (m, 1H), 3.0 (m, 3H), 3.36 (d, J = 10 Hz, 1H), 4.3 (br, 4H), 4.5 (m, 1H), 5.74 (s, 1H), 6.75 (s, 1H), 7.0–7.2 (m, 7H), 7.3 (m, 1H), 7.5 (m, 2H); FAB HRMS [$M + \text{H}]^+$ m/z 627.3175 (calcd for $\text{C}_{36}\text{H}_{43}\text{N}_4\text{O}_6$, 627.3182); TLC R_f 0.43 (15% methanol in dichloromethane).

[3-[(3(S)- or [3-[(3(R)-[Cyclopropyl[4-hydroxy-2-oxo-6-[1(R)-(phenylmethyl)propyl]-2H-pyran-3-yl]methyl]phenyl]amino]-1(S)-[(1H-imidazol-4-yl)methyl]-2-oxoethyl]carbamic acid *tert*-butyl ester (isomer 2 of **XXIV):** ^1H NMR (CDCl_3) δ 0.23 (m, 2H), 0.46 (m, 1H), 0.66 (m, 1H), 0.85 (t, J = 7.3 Hz, 3H), 1.40 (s, 9H), 1.61 (m, 2H), 1.9 (m, 1H), 2.50 (m, 1H), 2.8 (m, 1H), 3.0 (m, 3H), 3.36 (d, J = 10 Hz, 1H), 4.43 (m, 1H), 5.75 (s, 1H), 6.78 (s, 1H), 7.05 (m, 2H), 7.1–7.2 (m, 5H), 7.4–7.5 (m, 3H); FAB HRMS [$M + \text{H}]^+$ m/z 627.3175 (calcd for $\text{C}_{36}\text{H}_{43}\text{N}_4\text{O}_6$, 627.3182); TLC R_f 0.43 (15% methanol in dichloromethane).

[3-[(3(R)- or [3-[(3(S)-[Cyclopropyl[4-hydroxy-2-oxo-6-[1(S)-(phenylmethyl)propyl]-2H-pyran-3-yl]methyl]phenyl]amino]-1(S)-[(1H-imidazol-4-yl)methyl]-2-oxoethyl]carbamic acid *tert*-butyl ester (isomer 3 of **XXIV):** ^1H NMR (CDCl_3) δ 0.24 (m, 2H), 0.46 (m, 1H), 0.66 (m, 1H), 0.85 (t, J = 7.3 Hz, 3H), 1.38 (s, 9H), 1.61 (m, 2H), 1.9 (m, 1H), 2.49 (m, 1H), 2.8 (m, 1H), 3.0 (m, 3H), 3.37 (d, J = 10 Hz, 1H), 4.4 (br, 4H), 4.46 (m, 1H), 5.75 (s, 1H), 6.75 (s, 1H), 7.05 (m, 2H), 7.1–7.2 (m, 5H), 7.3–7.5 (m, 3H); FAB HRMS [$M + \text{H}]^+$ m/z 627.3181 (calcd for $\text{C}_{36}\text{H}_{43}\text{N}_4\text{O}_6$, 627.3182); TLC R_f 0.43 (15% methanol in dichloromethane).

[3-[(3(S)- or [3-[(3(R)-[Cyclopropyl[4-hydroxy-2-oxo-6-[1(S)-(phenylmethyl)propyl]-2H-pyran-3-yl]methyl]phenyl]amino]-1(S)-[(1H-imidazol-4-yl)methyl]-2-oxoethyl]carbamic acid *tert*-butyl ester (isomer 4 of **XXIV):** ^1H NMR (CDCl_3) δ 0.23 (m, 2H), 0.48 (m, 1H), 0.68 (m, 1H), 0.85 (t, J = 7.3 Hz, 3H), 1.40 (s, 9H), 1.6 (m, 2H), 1.9 (m, 1H), 2.5 (m, 1H), 2.8 (m, 1H), 3.0 (m, 3H), 3.36 (d, J = 10 Hz, 1H), 4.2 (br, 4H), 4.4 (m, 1H), 5.74 (s, 1H), 6.78 (s, 1H), 7.0–7.3 (m, 7H), 7.4–7.5 (m, 3H); FAB HRMS [$M + \text{H}]^+$ m/z 627.3181 (calcd for $\text{C}_{36}\text{H}_{43}\text{N}_4\text{O}_6$, 627.3182); TLC R_f 0.43 (15% methanol in dichloromethane).

Crystallography

Crystallization. The preparation and purification of the recombinant HIV-1 and HIV-2 proteases have been described elsewhere.³⁸ The protein preparation of HIV-2 protease contains a Lys57Leu mutation but has been found to be indistinguishable in activity and specificity from the wild type enzyme. The crystals of the proteases complexed with the selected inhibitors were obtained by cocrystallization experiments in which 2 mL of the inhibitor solution (of 0.1 mg/mL concentration) in DMSO was added to 130 μL of the freshly thawed ice-cold protease solution (ca. 6 mg/mL concentration) and the mixture equilibrated on ice for 30 min. The undissolved inhibitor that precipitates upon mixing was removed by centrifugation. In the case of the HIV-1 protease, crystals were grown at room temperature in 4–7 mL of hanging drops by vapor diffusion against a precipitant of 0.75–2.0 M NaCl at pH 4.8–5.2 (0.1 M acetate buffer) and pH 5.4–5.8 (0.1 M citrate buffer). In the case of the HIV-2 protease, they were grown against a precipitant of 30–35% (w/v) PEG 4000 in 0.1 HEPES, pH 6.8–7.6. Larger single crystals could occasionally be grown by addition of 1–3% *n*-butanol to the well solution.

Table 5. Summary of Selected Diffraction Data Collection and Refinement Statistics for the Four HIV Protease Inhibitor Complexes^a

inhibitor complex	HIV-1/III	HIV-2/V	HIV-2/XI	HIV-1/XX
space group	P6 ₁ 22	P2 ₁ 2 ₁ 2 ₁	P2 ₁ 2 ₁ 2 ₁	P2 ₁ 2 ₁ 2
unit cell				
<i>a</i> (Å)	63.47	33.73	34.02	59.26
<i>b</i> (Å)	63.47	46.46	46.00	87.21
<i>c</i> (Å)	84.10	135.52	134.18	46.19
resolution (Å)	2.2	1.9	2.5	3.0
no. of observations	31 369	55 194	21 608	30 558
unique reflections	4835	12 488	6651	5144
% complete	89	80	85	100
<i>R</i> _{merge}	0.140	0.111	0.068	0.149
<i>R</i> -factor (refinement)	0.178	0.173	0.208	0.164

^a Additional details may be found in the Brookhaven Protein Data Bank entries.

Data Collection. A single crystal of each was used for data collection in all cases. For the complexes of HIV-1/III, HIV-2/XI, and HIV-1/XX, diffraction data to 2.0 Å were collected using a Siemens area detector, with X-rays generated by a Siemens rotating anode source operating at 45 kV, 96 mA. Measurements were made as a series of 0.25° frames, with an exposure time of 240 s per frame. Data were collected on the HIV-2/V complex to a d spacing of 1.7 Å. Data sets were processed using the XENGEN data reduction software.³⁹ Table 5 summarizes the data collection statistics of the four data sets along with statistics from the refinement of the models. The effective resolution of each crystal was taken as the maximum resolution for which the mean *I*/*σ* was greater than 2.0 Å. Data beyond this maximum were discarded.

Structure Refinement. Since the space group of these protease/inhibitor complexes was the same as ones previously refined,^{38,40} refinement of these protease models could be initiated without resolving the position of the molecule in the cell. Initial structure refinements on the HIV-2/XI complex and the HIV-2/V complex were performed using the PROLSQ⁴¹ least-squares method with periodic manual rebuilding using FRODO interactive graphics,⁴² based on 2|*F*_o - *F*_c| and |*F*_o - *F*_c| electron density maps. Electron density maps were calculated using the XTAL package of crystallographic programs.⁴³ Refinement of the HIV-1/III and the HIV-1/XX complexes was carried out using CEDAR.⁴⁴ Diffraction data having intensities greater than 2σ were used in these calculations. Final refinements were carried out using CEDAR. The inhibitors and the solvent molecules were added during later stages of the refinements. The atomic coordinates of this structure are being deposited with the Protein Data Bank.⁴⁵ The HIV-2/XI complex was found in two overlapping orientations related by the pseudo 2-fold axis relating the two protein monomers. The HIV-2/V complex and the HIV-1/XX complex are found in only one orientation so that better structures of the inhibitor conformation could be determined. The HIV-2/V complex is one of our highest resolution structure determinations of an HIV-2 protease/inhibitor complex (1.9 Å resolution). The HIV-1/XX complex is not as well determined due to the 3.0 Å resolution crystallographic data cutoff.

HIV-1 Protease Inhibitory Assay and *K*_i Value Determination. HIV-1 protease was purified and refolded from *Escherichia coli* inclusion bodies.⁴⁶ The substrate used spans the p17-p24 processing site (R-V-S-Q-N-Y-P-I-V-Q-N-K) and was derivatized with bi-

otin and fluorescein isothiocyanate at the amino and carboxy termini, respectively. The reaction was performed in an assay buffer at substrate concentrations below *K*_m concentrations for 90 min at room temperature in the dark. The assay buffer consists of 0.1 M sodium acetate, 1.0 M NaCl, and 0.05% NP40. Enzyme and substrate concentrations are 10 and 50 nM, respectively. Inhibitors are dissolved in dimethyl sulfoxide, and the amount in the assay is 2%. After incubation, the reaction is stopped by addition of fluoricon avidin beads at 0.5% (w/v). The residual bound fluorescence is obtained by processing on an IDEXX Screen Machine, from which percent inhibition values are calculated. A range of inhibitor concentrations is used. Determination of *K*_i values with this assay requires analysis under conditions in which substrate concentration resides substantially below *K*_m and the inhibitor concentration greatly exceeds the *K*_i value and the enzyme concentration. One can solve the remaining substrate after prolonged incubation times as a quadratic, exponential function in terms of inhibitor concentrations and time to generate calculated values for the kinetic constants *K*_m, *k*_{cat}, and *K*_i as well as the enzyme concentration.

MTT Cytotoxicity Assay. Into appropriate wells of a 96-well microtiter plate was added 125 μL of 2× drug dissolved in RPMI complete medium, followed by 125 μL of a suspension of MT4 cells containing 2 × 10⁴ cells and mixed gently. Various drug concentrations were tested in triplicate. Positive controls contained cells and RPMI complete medium without drug, while negative controls contained medium only. Each microplate was incubated for 4–7 days at 37 °C in 5% CO₂. After completion of the incubation period, 100 μL of supernatant was removed, with minimal disturbance of the cells at the bottom of each well. To each well was added 10 μL of a freshly prepared MTT solution (5 mg/mL in PBS, Sigma). The plate was incubated for 4 h at 37 °C in 5% CO₂. An additional 50 μL was removed from all wells, and the cells were mixed thoroughly by vigorously pipetting up and down to resuspend the formazan dye precipitate. To each well was added 100 μL of 0.04 N HCl/isopropanol solution while the solution was mixed extensively. The plate was read within 15 min on a dual-wavelength microplate reader using a test wavelength of 570 nm and a reference wavelength of 650 nm. The cytotoxic activity of a test compound was calculated by dividing the mean OD at each drug concentration by the mean OD of the positive controls, subtracting the result from 1, and multiplying by 100. The CCTD₅₀ (cell culture toxicity dose₅₀) value was determined to be the calculated compound concentration required to inhibit 50% of cell metabolism when OD's between compound-exposed cells and compound-free control cells were compared. The CCTD₅₀ value was calculated by linear regression or by straight line extrapolation.

Antiviral Activity (MT4/HIV-1_{IIIB} Assay). MT4 cells were washed and resuspended in an inoculum of HIV-1_{IIIB} at a MOI of approximately 0.005. Adsorption occurred for 2 h at 37 °C in 5% CO₂. Unabsorbed virus was removed by low-speed centrifugation (200g, 10 min) of the cells followed by removal of the supernatant. The cell pellet was resuspended to a concentration of 8 × 10⁵ cells/mL in RPMI complete medium. In appropriate wells of 24-well tissue culture plates (Corning Catalog no. 25820), 0.5 mL of infected MT4 cells and 0.5 mL of

2× test compound dissolved in RPMI complete medium plus 0.2% DMSO were combined. Each drug concentration was tested in triplicate. Virus control wells received RPMI complete medium plus 0.2% DMSO without compound. The final DMSO concentration in each culture was 0.1%. Plates were incubated for 7 days at 37 °C in 5% CO₂. At the end of the 7 day incubation period, 100 μL of supernatant was removed from each test well and live virus inactivated by the addition of lysis buffer (Coulter Diagnostics, Hialeah, FL) containing 5% Triton X-100. The amount of HIV p24 core antigen was quantified with an ELISA procedure by following the manufacturer's direction. The IC₅₀ (inhibitory concentration₅₀), the amount of drug necessary to reduce the concentration of p24 in drug-containing cultures by 50% when compared to drug-free controls, was calculated by comparing the quantity of p24 produced in drug-containing cultures with that of DMSO-containing drug-free supernatants. This was accomplished by using the linear portion of the plot of log₁₀ drug concentration versus percent p24 inhibition and utilizing linear regression or straight line extrapolation to calculate the drug concentration necessary to inhibit 50% of nondrug-treated p24 antigen.

Acknowledgment. We gratefully acknowledge Carol A. Bannow and Linda L. Maggiora for the preparation of the biotinylated and fluorescent-labeled substrate for the enzyme inhibitory assay.

References

- (1) Blundell, T. L.; Lapatto, R.; Wilderspin, A. F.; Hemmings, A. M.; Hobart, P. M.; Danley, D. E.; Whittle, P. J. The 3-D Structure of HIV-1 Protease and the Design of Antiviral Agents for the Treatment of AIDS. *Trends Biochem. Sci.* **1990**, *15*, 425–430.
- (2) Debouck, C.; Metcalf, B. W. Human Immunodeficiency Virus Protease: A Target for AIDS Therapy. *Drug Dev. Res.* **1990**, *21*, 1–17.
- (3) Huff, J. R. HIV Protease: A Novel Chemotherapeutic Target for AIDS. *J. Med. Chem.* **1991**, *34*, 2305–2314.
- (4) Meek, T. D. Inhibitors of HIV-1 Protease. *J. Enzyme Inhib.* **1992**, *6*, 65–98.
- (5) Robins, T.; Plattner, J. HIV Protease Inhibitors: Their Anti-HIV Activity and Potential Role in Treatment. *J. Acquired Immune Defic. Syndr.* **1993**, *6*, 162–170.
- (6) Thaisrivongs, S. Chapter 14. HIV Protease Inhibitors. *Annu. Rep. Med. Chem.* **1994**, *29*, 133–144.
- (7) Plattner, J. J.; Norbeck, D. W. Obstacles to Drug Development from Peptide Leads. In *Drug Discovery Technologies*; Clark, C. R., Moos, W. H., Eds.; Ellis Horwood Ltd.: Chichester, U.K., 1990; Chapter 5, pp 92–126.
- (8) Martin, J. A. Recent Advances in the Design of HIV Protease Inhibitors. *Antiviral Res.* **1992**, *17*, 265–278.
- (9) Kempf, D. J.; Codacovi, L.; Wang, X. C.; Kohlbrenner, W. E.; Wideburg, N. E.; Saldivar, A.; Vasavanonda, S.; Marsh, K. C.; Bryant, P.; Sham, H. L.; Green, B. E.; Betebeben, D. A.; Erickson, J.; Norbeck, D. W. Symmetry-based Inhibitors of HIV Protease. Structure-Activity Studies of Acylated 2,4-Diamino-1,5-diphenyl-3-hydroxypentane and 2,5-Diamino-1,6-diphenylhexane-3,4-diol. *J. Med. Chem.* **1993**, *36*, 320–330.
- (10) Kempf, D. J.; Marsh, K. C.; Fino, L. C.; Bryant, P.; Craig-Kennard, A.; Sham, H. L.; Zhao, C.; Vasavanonda, S.; Kohlbrenner, W. E.; Wideburg, N. E.; Saldivar, A.; Green, B. E.; Herrin, T.; Norbeck, D. W. Design of Orally Bioavailable, Symmetry-based Inhibitors of HIV Protease. *Bioorg. Med. Chem.* **1994**, *2*, 847–858.
- (11) Kempf, D. J.; Marsh, K. C.; Denissen, J. F.; McDonald, E.; Vasavanonda, S.; Flentge, C. A.; Green, B. E.; Fino, L.; Park, C. H.; Kong, X.-P.; Wideburg, N. E.; Saldivar, A.; Ruiz, L.; Kati, W. M.; Sham, H. L.; Robins, T.; Stewart, K. D.; Hsu, A.; Plattner, J. J.; Leonard, J. M.; Norbeck, D. W. ABT-538 is a Potent Inhibitor of Human Immunodeficiency Virus Protease and has High Oral Bioavailability in Humans. *Proc. Natl. Acad. Sci. U.S.A.* **1995**, *92*, 2484–2488.
- (12) Vacca, J. P.; Dorsey, B. D.; Schleif, W. A.; Levin, R. B.; McDaniel, S. L.; Darke, P. L.; Zugay, J.; Quintero, J. C.; Blahy, O. M.; Roth, E.; Sardana, V. V.; Schlabbach, A. J.; Graham, P. I.; Condra, J. H.; Gotlib, L.; Holloway, M. K.; Lin, J.; Chen, I.-W.; Vastag, K.; Ostovic, D.; Anderson, P. S.; Emini, E. A.; Huff, J. R. L-735-524: An Orally Bioavailable Human Immunodeficiency Virus Type 1 Protease Inhibitor. *Proc. Natl. Acad. Sci. U.S.A.* **1994**, *91*, 4096–4100.
- (13) Lam, P. Y.-S.; Jadhav, P. K.; Eyermann, C. J.; Hodge, C. N.; Ru, Y.; Bacheler, L. T.; Meek, J. L.; Otto, M. J.; Rayner, M. M.; Wong, Y. N.; Chang, C.-H.; Weber, P. C.; Jackson, D. A.; Sharpe, T. R.; Erickson-Vitanen, S. Rational Design of Potent, Bioavailable, Non-peptide Cyclic Urea as HIV Protease Inhibitors. *Science* **1994**, *263*, 380–384.
- (14) Wong, Y. N.; Burcham, D. L.; Saxton, P. L.; Erickson-Vitanen, S.; Grubb, M. F.; Quon, C. Y.; Huang, S.-M. A Pharmacokinetic Evaluation of HIV Protease Inhibitors, Cyclic Ureas, in Rats and Dogs. *Biopharm. Drug Dispos.* **1994**, *15*, 535–544.
- (15) Getman, D. P.; DeCrescenzo, G. A.; Heintz, R. M.; Reed, K. L.; Talley, J. J.; Bryant, M. L.; Clare, M.; Houseman, K. A.; Marr, J. J.; Mueller, R. A.; Vazquez, M. L.; Shieh, H.-S.; Stallings, W. C.; Stegeman, R. A. Discovery of a Novel Class of Potent HIV-1 Protease Inhibitors Containing the (R)-(Hydroxyethyl)urea Isostere. *J. Med. Chem.* **1993**, *36*, 288–291.
- (16) Bryant, M. HIV Protease Inhibitors: Action to Efficacy. Inhibitor SC-55389a presented at Session 46 (I) at the 34th Inter-science Conference on Antimicrobial Agents and Chemotherapy, Orlando, FL, 1994.
- (17) Kim, E. E.; Baker, C. T.; Dwyer, M. D.; Murcko, M. A.; Rao, B. G.; Tung, R. D.; Navia, M. A. Crystal Structure of HIV-1 Protease in Complex with VX-478, a Potent and Orally Bioavailable Inhibitor of the Enzyme. *J. Am. Chem. Soc.* **1995**, *117*, 1181–1182.
- (18) Shetty, B.; Kaldor, S.; Kalish, V.; Reich, S.; Webber, S. AG1343, An Orally Bioavailable Non-Peptidic HIV-1 Protease Inhibitor. Presented at the 10th International Conference on AIDS, Yokohama, Japan, 1994; Abstract 321A.
- (19) Mimoto, T.; Imai, J.; Kisanuki, S.; Enomoto, H.; Hattori, N.; Akaju, K.; Kiso, Y. Kynostatin KNI-227 and -272, Highly Potent Anti-HIV Agents: Conformationally Constrained Tripeptide Inhibitors of HIV Protease Containing Allophenylnorstatine. *Chem. Pharm. Bull.* **1992**, *40*, 2251–2253.
- (20) Thaisrivongs, S.; Tomich, P. K.; Watenpaugh, K. D.; Chong, K. T.; Howe, W. J.; Yang, C.-P.; Strohbach, J. W.; Turner, S. R.; McGrath, J. P.; Bohanon, M. J.; Lynn, J. C.; Mulichak, A. M.; Spinelli, P. A.; Hinshaw, R. R.; Pagano, P. J.; Moon, J. B.; Ruwart, M. J.; Wilkinson, K. F.; Rush, B. D.; Zipp, G. L.; Dalga, R. J.; Schwende, F. J.; Howard, G. M.; Padbury, G. E.; Toth, L. N.; Zhao, Z.; Koeplinger, K. A.; Kakuk, T. J.; Cole, S. L.; Zaya, R. M.; Piper, R. C.; Jeffrey, P. Structure-Based Design of HIV Protease Inhibitors: 4-Hydroxycoumarins and 4-Hydroxy-2-pyrones as Non-peptidic Inhibitors. *J. Med. Chem.* **1994**, *37*, 3200–3204.
- (21) Ashorn, P.; McQuade, T. J.; Thaisrivongs, S.; Tomasselli, A. G.; Tarpley, W. G.; Moss, B. An Inhibitor of the Protease Blocks Maturation of Human and Simian Immunodeficiency Viruses and Spread of Infection. *Proc. Natl. Acad. Sci. U.S.A.* **1990**, *87*, 7472–7476.
- (22) Thaisrivongs, S.; Tomasselli, A. G.; Moon, J. B.; Hui, J.; McQuade, T. J.; Turner, S. R.; Strohbach, J. W.; Howe, W. J.; Tarpley, W. G.; Heinrikson, R. L. Inhibitors of the Protease from Human Immunodeficiency Virus: Design and Modeling of a Compound Containing a Dihydroxyethylene Isostere Insert with High Binding Affinity and Effective Antiviral Activity. *J. Med. Chem.* **1991**, *34*, 2344–2356.
- (23) Martin, L. N.; Soite, K. F.; Murphy-Corb, M.; Bohm, R. P.; Roberts, E. D.; Kakuk, T. J.; Thaisrivongs, S.; Vidmar, T. J.; Ruwart, M. J.; Davio, S. R.; Tarpley, W. G. Effects of U-75875, a Peptidomimetic Inhibitor of Retroviral Protease, on Simian Immunodeficiency Virus Infection in Rhesus Monkeys. *Antimicrob. Agents Chemother.* **1994**, *38*, 1277–1283.
- (24) Bourinbaiar, A. S.; Tan, X.; Nagorny, R. Effect of the Oral Anticoagulant, Warfarin, on HIV-1 Replication and Spread. *AIDS* **1993**, *7*, 129–130.
- (25) Tummino, P. J.; Ferguson, D.; Hupe, L.; Hupe, D. Competitive Inhibition of HIV-1 Protease by 4-Hydroxy-benzopyran-2-ones and by 4-Hydroxy-6-phenylpyran-2-ones. *Biochem. Biophys. Res. Commun.* **1994**, *200*, 1658–1664.
- (26) Tummino, P. J.; Ferguson, D.; Hupe, D. Competitive Inhibition of HIV-1 Protease by Warfarin Derivatives. *Biochem. Biophys. Res. Commun.* **1994**, *201*, 290–294.
- (27) Vara Prasad, J. V. N.; Para, K. S.; Lunney, E. A.; Ortwine, D. F.; Dunbar, J. B., Jr.; Ferguson, D.; Tummino, P. J.; Hupe, D.; Tait, B. D.; Domagala, J. M.; Humblet, C.; Bhat, T. N.; Liu, B.; Guerin, D. M. A.; Baldwin, E. T.; Erickson, J. W.; Sawyer, T. K. Novel Series of Achiral, Low Molecular Weight, and Potent HIV-1 Protease Inhibitors. *J. Am. Chem. Soc.* **1994**, *116*, 6989–6990.
- (28) Lunney, E. A.; Hagen, S. E.; Domagala, J. M.; Humblet, C.; Kosinski, J.; Tait, B. D.; Warmus, J. S.; Wilson, M.; Ferguson, D.; Hupe, D.; Tummino, P. J.; Baldwin, E. T.; Bhat, T. N.; Liu, B.; Erickson, J. W. A Novel Nonpeptide HIV-1 Protease Inhibitor: Elucidation of the Binding Mode and Its Application in the Design of Related Analogs. *J. Med. Chem.* **1994**, *37*, 2664–2677.

- (29) Wlodawer, A.; Erickson, J. W. Structure-based Inhibitors of HIV-1 Protease. *Annu. Rev. Biochem.* **1993**, *62*, 543–585.
- (30) Appelt, K. Crystal Structures of HIV-1 Protease-Inhibitor Complexes. *Perspect. Drug Discovery Des.* **1993**, *1*, 23–48.
- (31) Thanki, N.; Rao, J. K. M.; Foundling, S. I.; Howe, W. J.; Moon, J. B.; Hui, J. O.; Tomasselli, A. G.; Heinrikson, R. L.; Thairivongs, S.; Wlodawer, A. Crystal Structure of a Complex of HIV-1 Protease with a Dihydroxyethylene-containing Inhibitor: Comparison with Molecular Modeling. *Protein Sci.* **1992**, *1*, 1061–1072.
- (32) S_n to S_{n'} refers to the nomenclature for enzyme-binding pockets as described in: Schechter, I.; Berger, A. On the Size of the Active Site in Proteases. I. Papain. *Biochem. Biophys. Res. Commun.* **1967**, *27*, 157–162.
- (33) Moon, J. B.; Howe, W. J. Computer Design of Bioactive Molecules: A Method for Receptor-Based de Novo Ligand Design. *Proteins: Struct., Funct., Genet.* **1991**, *11*, 314–328.
- (34) Mossmann, T. Rapid Colorimetric Assay for Cellular Growth and Survival: Application to Proliferation and Cytotoxicity Assays. *J. Immunol. Methods* **1983**, *65*, 55–63.
- (35) Chong, K.-T.; Pagano, P. J.; Hinshaw, R. R. Bisheteroarylpiperazine Reverse Transcriptase Inhibitor in Combination with 3'-Azido-3'-Deoxythymidine or 2',3'-Dideoxycytidine Synergistically Inhibits Human Immunodeficiency Virus Type 1 Replication In Vitro. *Antimicrob. Agents Chemother.* **1994**, *38*, 288–293.
- (36) Lyle, T. A.; Wiscount, C. M.; Guare, J. P.; Thompson, W. J.; Anderson, P. S.; Darke, P. L.; Zugay, J. A.; Emini, E. A.; Schleif, W. A.; Quintero, J. C.; Dixon, R. A. F.; Sigal, I. S.; Huff, J. R. Bicycloalkyl Amines as Novel C-termini for HIV Protease Inhibitors. *J. Med. Chem.* **1991**, *34*, 1228–1230.
- (37) Harris, T. M.; Harris, C. M. Carboxylation of β-Dicarbonyl Compounds through Dicarbanions. Cyclizations to 4-Hydroxy-2-pyrones. *J. Org. Chem.* **1966**, *31*, 1032–1035.
- (38) Mulichak, A. M.; Hui, J. O.; Tomasselli, A. G.; Heinrikson, R. L.; Curry, K. A.; Tomich, C.-S.; Thairivongs, S.; Sawyer, T. K.; Watenpaugh, K. D. The Crystallographic Structure of the Protease from Human Immunodeficiency Virus Type 2 with Two Synthetic Peptide Transition State Analog Inhibitors. *J. Biol. Chem.* **1993**, *268*, 13103–13109.
- (39) Howard, A. J.; Gilliland, G. L.; Finzel, B. C.; Poulos, T. L.; Ohlendorf, D. H.; Salemme, F. R. The Use of an Imaging Proportional Counter in Macromolecular Crystallography. *J. Appl. Crystallogr.* **1987**, *20*, 383–387.
- (40) Tomasselli, A. G.; Howe, W. J.; Sawyer, T. K.; Wladawer, A.; Heinrikson, R. L. The Complexities of AIDS: An Assessment of the HIV Protease as a Therapeutic Target. *Chim. Oggi* **1991**, *9*, 6–27.
- (41) Hendrickson, W. A.; Konnert, J. H. Stereochemically Restrained Crystallographic Least-squares Refinement of Macromolecule Structures. In *Biomolecular Structure, Function and Evolution*; Srinivasan, R., Ed.; Pergamon Press: Oxford, 1980; pp 43–57.
- (42) Jones, T. A. Interactive Computer Graphics: FRODO. *Methods Enzymol.* **1985**, *115*, 157–171.
- (43) Hall, S. R., Stewart, J. M., Eds. Xtal 3.0 Reference Manual; University of Western Australia and University of Maryland: Perth, Australia, and College Park, MD, 1990.
- (44) Watenpaugh, K. D. Conformational Energy as a Restraint in Refinement. In *Proceeding of the Molecular Dynamics Workshop, 1984*, Chapel Hill; Hermans, J., Ed.; Polycrystal Book: Western Springs, IL, 1985; pp 77–80.
- (45) Bernstein, F. C.; Koetzle, T. F.; Williams, G. J. B.; Meyer, E. F.; Brice, M. D.; Rogers, J. B.; Kennard, O.; Shimanouchi, T.; Tasumi, M. The Protein Data Bank: A Computer-based Archival File for Macromolecular Structures. *J. Mol. Biol.* **1977**, *112*, 535–542.
- (46) Tomasselli, A. G.; Olsen, M. K.; Hui, J. O.; Staples, D. J.; Sawyer, T. K.; Heinrikson, R. L.; Tomich, C.-S. C. Substrate Analogue Inhibition and Active Site Titration of Purified Recombinant HIV-1 Protease. *Biochemistry* **1990**, *29*, 264–269.

JM950296X